



# Concentrating photovoltaic systems: a review of temperature effects and components

Yuan Zou<sup>1</sup> · Caiyan Qin<sup>2</sup> · Haotuo Liu<sup>3</sup> · Bin Zhang<sup>1</sup> · Xiaohu Wu<sup>3</sup>

Received: 5 July 2023 / Accepted: 13 November 2023 / Published online: 11 December 2023  
© Akadémiai Kiadó, Budapest, Hungary 2023

## Abstract

Concentrating photovoltaic (CPV) technology is a promising approach for collecting solar energy and converting it into electricity through photovoltaic cells, with high conversion efficiency. Compared to conventional flat panel photovoltaic systems, CPV systems use concentrators solar energy from a larger area into a smaller one, resulting in a higher density of solar radiation and increased electrical output. However, the use of concentrators can lead to nonuniform radiation and high temperatures that may damage the solar cells. Therefore, implementing a suitable thermal management solution is crucial to ensure optimal performance of CPV systems. This review article aims to provide a comprehensive overview of recent research and technical challenges in solar concentrators, trackers, and cooling systems for mitigating temperature effects and enhancing the efficiency of CPV cells. It will explore the causes and potential solutions for temperature effects in CPV systems, particularly focusing on the components involved.

**Keywords** Concentrating photovoltaic system · Temperature effect · Solar concentrators · Solar trackers · Cooling systems

## Abbreviations

a-Si	Amorphous silicon
A.R.	Area ratio
CIGS	Copper indium gallium selenide
CdTe	Cadmium telluride
CO <sub>2</sub>	Carbon dioxide
CPVD	Daylighting window
CPV	Concentrating photovoltaic
CPV/T	Concentrating photovoltaic/thermal
CPV/TEG	Concentrating photovoltaic/ thermoelectric generator
CLFR	Compact linear Fresnel reflector
EMR	Eliminating multiple reflections
FL	Fresnel

HCPV	High concentrating photovoltaic
LCPV	Low concentrating photovoltaic
LCPV/T	Low concentrating photovoltaic/thermal
LSC	Luminescent solar concentrator
m-Si	Monocrystalline silicon
NCPV/T-TEG	Nanofluid concentrating photovoltaic/ thermal-thermoelectric generator
OVSC	New V-trough solar concentrator
OHP	Oscillating heat pipe
p-Si	Polycrystalline Silicon
Si	Silicon
SiC	Silicon carbide
TMPL	Two-phase mechanical pump loop
TEG	Thermoelectric generator

## Greek symbols

$\delta$	The angle between the incident center line of sunlight and Z-axis
$\mu$	Solar flux distribution uniformity factor
$\overline{\sigma}_m$	: Monthly mean effective tracking factor
$\overline{\sigma}_y$	: Annual mean effective tracking factor

✉ Bin Zhang  
zb-sh@163.com

✉ Xiaohu Wu  
xiaohu.wu@iat.cn

<sup>1</sup> College of Electromechanical Engineering, Qingdao University of Science and Technology, Qingdao 266061, China

<sup>2</sup> School of Mechanical Engineering and Automation, Harbin Institute of Technology, Shenzhen 518055, China

<sup>3</sup> Shandong Institute of Advanced Technology, Jinan 250100, China

## Introduction

The 26th Conference of the Parties (COP26) acknowledged that nations worldwide continue to confront climate and environmental challenges [1, 2]. The primary driver behind global climate change remains the excessive release of greenhouse gases, notably CO<sub>2</sub> [3–5]. Fossil fuel combustion predominantly contributes to the emission of these gases; however, thermal power generation alone accounts for approximately 42% of global CO<sub>2</sub> emissions [6–9]. Therefore, an urgent quest for environmentally sustainable and clean energy sources is imperative in mitigating CO<sub>2</sub> emissions and addressing climate change concerns [10, 11].

Renewable energy development is crucial to achieving a low-carbon economy [12–14]. Among the various renewable energy sources, solar energy has garnered significant attention from researchers due to its cost-free nature, environmentally friendly, and without geographical restrictions [7, 15]. Since Becquerel first discovered the photovoltaic effect [16], solar energy has demonstrated immense potential for electricity production. Over the years of research, photovoltaic power generation has been gradually transitioned from high-cost first-generation crystalline silicon (Si) cells to lower-cost second-generation thin-film cells, third-generation organic solar cells, and dye-sensitized solar cells, among others [7, 17, 18]. It has been reported that photovoltaic power could contribute significantly to emission reduction potential by 2050 [19]. However, photovoltaic systems still suffer from drawbacks such as low power generation efficiency and high cost [20, 21].

The concentrating photovoltaic (CPV) systems are the technology that directly converts concentrated sunlight into power through photovoltaic cells, achieving high conversion efficiency [22, 23]. The diagram in Fig. 1 presents an overview of a CPV system, using a reflective condenser as an illustrative example. This system employs a concentrator to condense a larger area of solar energy onto a smaller surface, thereby providing higher sunlight intensity to the solar cells at specific locations. By utilizing low-cost reflectors/lenses

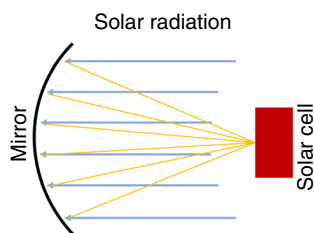


**Fig. 1** Overview of the concentrating photovoltaic system (Take the reflective condenser as an example)

instead of expensive photovoltaic materials, CPV systems aim to reduce the overall cost of photovoltaic systems while addressing the issue of low density in solar radiation energy flow and obtain more power output [24, 25].

In CPV systems, the concentration ratio serves as a metric for assessing the incident radiation intensity on a solar cell under concentration. Based on concentration ratio intensity, CPV systems are categorized into low, medium, and high concentrating photovoltaic (LCPV, MCPV, HCPV). The light-harvesting capacity of a CPV system is determined by the [26]. While higher concentration ratios can reduce material requirements for solar cells, they also increase power generation costs and exacerbate temperature effects on solar cell efficiency [22]. Consequently, CPV systems still face two primary challenges: nonuniform radiation [27] and elevated temperatures resulting from high radiation exposure [28].

The CPV system primarily consists of a photoelectric converter, a concentrator system, and a balance system [29]. Among these components, the solar cell serves as the device responsible for converting solar energy into electricity, representing the core part of photovoltaic power generation [30]. However, it is worth noting that the efficiency and temperature of the CPV system are predominantly influenced by the concentrator. Consequently, to prevent any degradation in optical and cell efficiency levels [31], solar tracking and cooling systems are often required in CPV systems. Several measures can typically be implemented:

- Adding cooling systems;
- Adding solar tracking systems;
- Optimization/development of solar concentrators;
- Establishment of coupled systems for thermoelectric power generation.

A comprehensive understanding of CPV system components is crucial for addressing the temperature effects of CPV systems. Therefore, this work aims to provide a comprehensive review of strategies for mitigating the temperature effect (including nonuniform radiation and high temperature) of CPV systems from three perspectives: solar concentrator (in “[Solar concentrators](#)” section), solar tracker (in “[Solar tracker](#)” section), and cooling system (in “[Cooling systems](#)” section), as illustrated in Fig. 2.

In addition, Table 1 also provides a comprehensive summary of the most notable review papers published in recent years. It is worth noting that the majority of these reviews primarily focus on investigating specific aspects, such as the impact of temperature distribution on cells [32], concentrating technology [20, 33], and solar cells [25]. However, to date, no researcher has conducted a comprehensive review specifically examining the temperature effects of CPV systems from the perspective

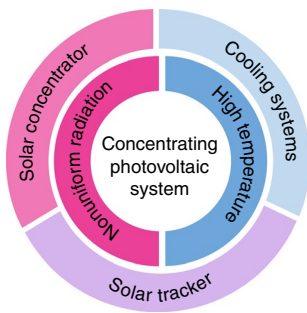


**Fig. 2** The schematic diagram illustrating the challenges and solutions encountered by the temperature impact on concentrating photovoltaic systems in this review

of CPV components. Therefore, this work will contribute to a comprehensive understanding and in-depth analysis of the latest advancements and emerging trends pertaining to temperature effects in CPV systems.

### Solar concentrators

The concentrator is an optical device that efficiently collects sunlight onto a small area, thereby increasing the energy density of solar radiation [38]. On the one hand, the concentrator in the CPV system enables high-performance solar cells to receive concentrated sunlight on a smaller surface area, enhancing the overall energy density. On the other hand, inexpensive concentrators can be utilized as substitutes for costly solar cell materials to effectively reduce the cost of photovoltaic power generation systems [39]. Additionally, it serves as the primary determinant of temperature nonuniformity in CPV systems. Enhancing the existing concentrator or developing novel ones can effectively of nonuniform radiation in CPV systems. Table 2 summarizes four common types of concentrators and their characteristics in concentrating photovoltaic systems. It is noteworthy that

there are variations in the features of different concentrators with respect to relative cost, operating temperature, and concentration ratio. The identification/selection of appropriate concentrators under specific conditions is critical for concentrating photovoltaic systems. Hence, this section presents a comprehensive review of recent research advancements, encompassing Fresnel concentrators, Dish concentrators, Composite Parabolic Trough concentrators, and Trough concentrators.

### Fresnel concentrators

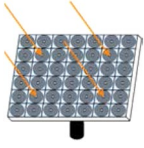
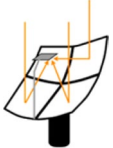
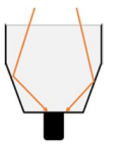

Fresnel (FL) concentrators are extensively utilized in CPV systems [43]. The continuous progress in manufacturing technology and the development of novel synthetic materials have prompted a re-examination of FL after nearly a century. Apart from their traditional use in lighthouses, FL applications have expanded significantly to encompass diverse fields such as lighting [44], communication [45], and printing technology [46]. The excellent optical properties and cost-effectiveness of FL have led to its proposed application in solar photovoltaics, resulting in a series of extensive studies. Due to its compact size light-mass nature, large-scale production capability, affordability, and high energy density [43], FL has emerged as one of the most promising options for concentrated solar energy applications. The schematic diagram of a linear Fresnel reflector (LFR) as a concentrator in a CPV system is illustrated in Fig. 3. Upon incidence, solar rays are redirected by the LFR concentrator toward the surface of the solar cell.

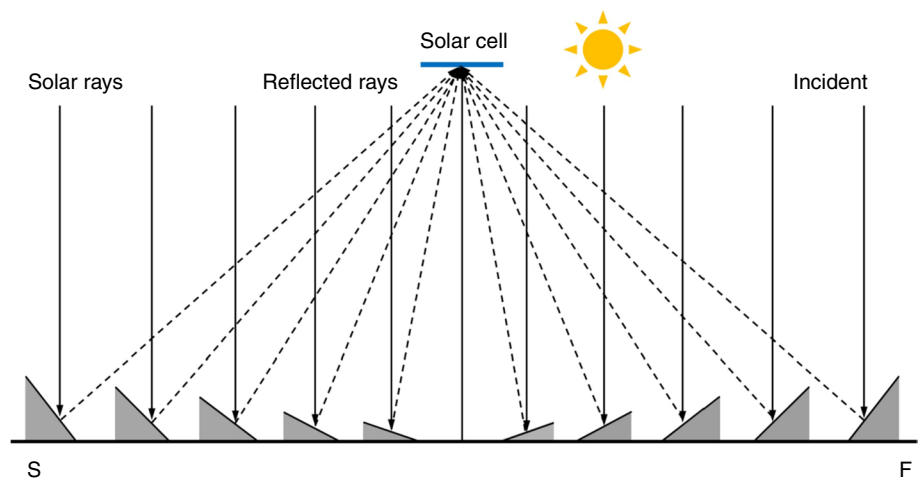
Vu et al. [48] proposed a cylindrical Fresnel lens inspired by the design of a Fresnel lighthouse, which demonstrated an optimal configuration that can increase the concentrator ratio to nearly 21 with an optical efficiency of 70%. Compared to a flat Si panel under identical sunlight conditions, this CPV system based on such a concentrator increased power output by 1.3 times. The linear Fresnel reflector solar concentrator (LFRSC) comprises three main components:

**Table 1** A review of the last 5 years of research on concentrating photovoltaic systems

Refs.	Year	The main content of the review
Li et al. [32]	2018	The effects of inhomogeneous light and temperature distributions on concentrating solar cells
Hasan et al. [20]	2018	Reviewed the thermal issues of different CPV systems and concentrating technologies
Alamoudi et al. [33]	2019	Reviewed the latest technological developments in static photovoltaic concentrators
Alves et al. [25]	2020	Reviewed the current status of the preparation of thin-film solar cells in CPV systems
Gharzi et al. [34]	2020	Reviewed the cooling techniques for concentrating photovoltaic modules
Tina et al. [35]	2021	Reviewed the research on machine learning in the field of photovoltaic systems
Ziemińska-Stolarska et al. [36]	2021	Reviewed the application of LCA in the determination of the environmental impact of concentrating solar panels
Ejaz et al. [22]	2021	Reviewed the progress and prospects of concentrated photovoltaic systems for light harvesters
Ibrahim et al. [37]	2023	Reviewed pulsating flow cooling in CPV cooling systems

**Table 2** Classification and characteristics of solar concentrators [40–42]

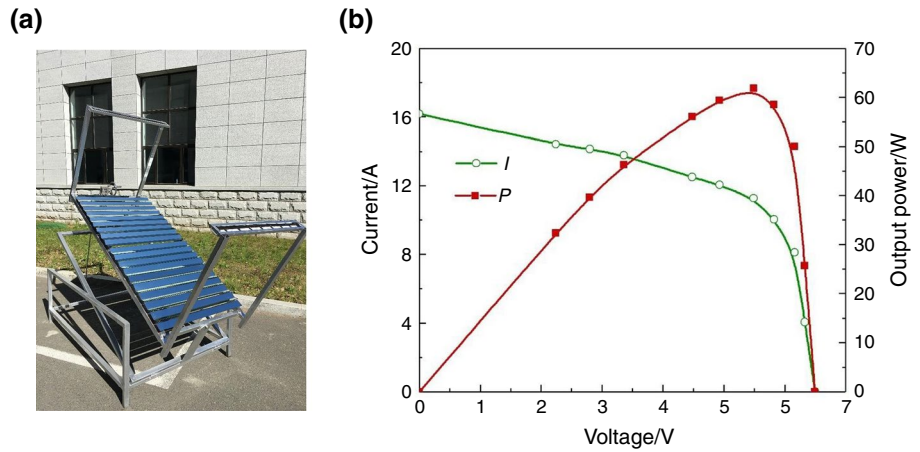
Solar concentrators	Relative cost	Operating Temperature range/°C	Solar concentration ratio	Improvement potential
Fresnel 	Very low	50–300	10–40	Significant
Dish 	Very high	120–1500	100–1000	High potential
Compound parabolic 	Low	100–150	3–10	Very significant
Trough 	Low	20–400	15–45	Limited

**Fig. 3** Schematic diagram of the concentrating photovoltaic device with the linear Fresnel reflector concentrator [47]

the primary mirror, secondary reflector, and absorber tube; however, achieving superior performance requires more efficient primary and secondary mirrors than conventional ones. Ahmadpour et al. [49] optimized the LFRSC structure for higher efficiency in three cases: small (Case I), medium (Case II), and optimized (Case III). The study findings indicate that Case III represents the optimal output efficiency configuration, achieving full optimization.

However, Case II cases in terms of manufacturing cost and simplicity. Wang et al. [50] proposed a CPV system with a compact linear Fresnel reflector (CLFR) concentrator is shown in Fig. 4a. The results demonstrate that the CLFR exhibits the highest degree of uniformity in concentrated solar radiation, while the CLFR-CPV system can achieve a photovoltaic conversion efficiency of 15.9%, as shown in Fig. 4b. Alamri et al. [51] proposed the potential of a novel

**Fig. 4 a** Diagram of the experimental setup of the concentrating photovoltaic system based on full-type compact linear Fresnel reflector; **b**  $I$ - $V$  characteristics test results of the photovoltaic cell module [50]



integrated CPV system, comprising an FL concentrator as the primary optical element, a multi-branch homogenizer as the secondary optical element (SOE), a planoconcave lens, and four Multi-junction solar cells. The study results show that the irradiance uniformity of the refractive index homogeneity surpasses than that of the reflective index homogeneity. Wu et al. [52] developed a multi-physics model that integrates optical, thermal, electrical, and structural models using MCRT-FVM-FEM to accurately determine the installation position of concentrators. They investigated the impact of concentrator placement on the thermal, electrical, and structural properties of photovoltaic panels. The results indicate that significant variations in these properties occur when  $\alpha = 75^\circ$ . However, the flow and temperature fields near the photovoltaic panel are minimal impact on concentrator placement.

**Dish concentrators**

The popularization and application of the traditional Dish system need to be improved due to its large size, complex structure, and high cost [53]. Therefore, Zheng et al. [54] proposed a novel ultralight Dish system consisting of a cable mesh reflector, an ultralight thermoelectric converter, and a triple telescopic rod (TER) solar tracker. This innovative system demonstrates advantages such as low cost, simplified fabrication process, and convenient transportation. Additionally, to achieve a uniform distribution of light intensity for highly efficient triple-junction solar CPV modules, Lokeswaran et al. [55] proposed the design of a two-stage square CPV receiver with a total geometric concentration ratio of 500-Suns, as depicted in Fig. 5a. The main research results are shown in Fig. 5b. The optical module achieves a maximum efficiency of 68 CPV module reaches an efficiency of 32.03%. These efficiencies are obtained when the homogenizer length is set at 0.005 m, and the receiver height

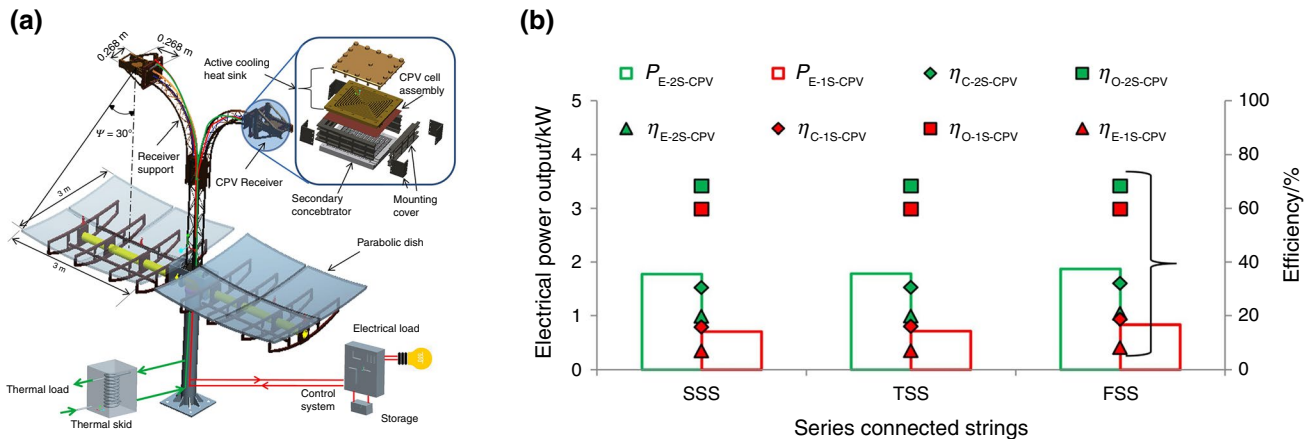


**Fig. 5 a** Schematic diagram of a square parabolic dish-based concentrating photovoltaic receiver; **b** Effect of tube string connection on output power, optics, concentrating photovoltaic, and electrical efficiency of two stage concentrating photovoltaic and conventional single stage receivers [55]

ciency of two stage concentrating photovoltaic and conventional single stage receivers [55]

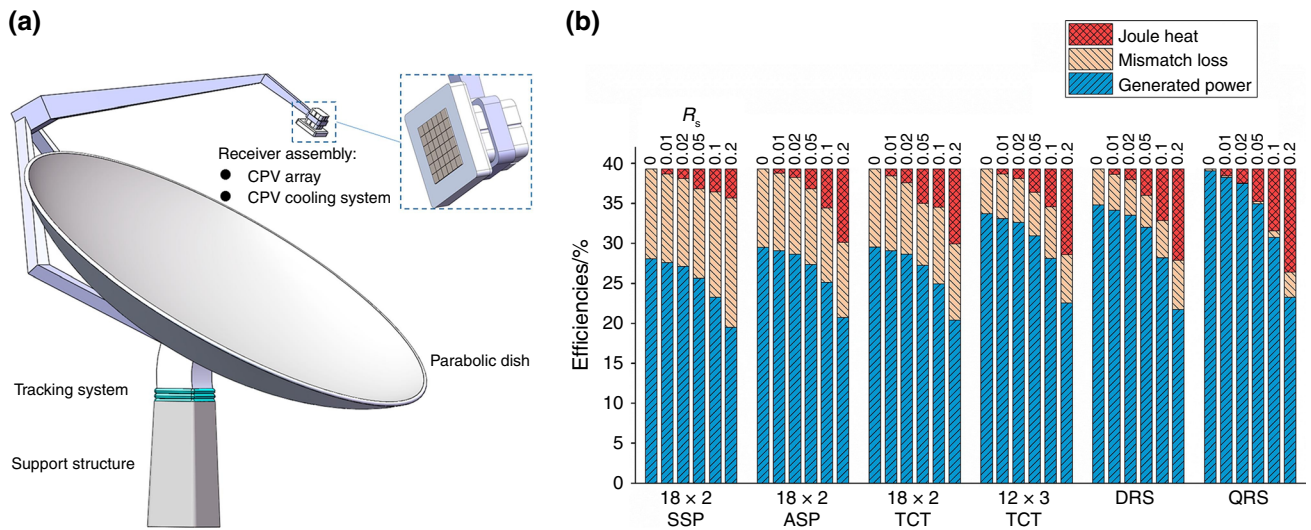


**Fig. 6** **a** Schematic diagram of the dense-array concentrator photovoltaic system; **b** The percentage of Joule heat, mismatch loss and power to the total energy of different series resistors when the total error of irradiance distribution is 4 [56]

is maintained at 3.7 m. Remarkably, this developed CPV system generates an annual electricity output of 2.19 MWh, representing a significant improvement of 33.54% compared to conventional systems. To reduce significant mismatch loss caused by nonuniform radiation, Pan et al. [56] developed a novel connection method for dense-array concentrating photovoltaic (DA-CPV) modules based on the dish Concentrating Photovoltaic system, as illustrated in Fig. 6a. As shown in Fig. 6b, the conversion efficiency of dichotomic rotational symmetry (DRS) and quartered rotational symmetry (QRS) connections is improved by 48% and 64.3%, respectively, compared to the conventional series–parallel (SP) connections.

Thirunavukkarasu et al. [57] studied the energy and exergy analysis of solar parabolic disk concentrator external spiral tube receivers under three different radiation conditions. The study findings reveal that the receiver achieves an average thermal efficiency of 56.21% and exergy efficiency of 5.45%, respectively, under an average beam radiation intensity of  $750 \text{ W m}^{-2}$ . Moreover, the receiver demonstrates a light-mass design and cost-effectiveness, making it a promising candidate for process heating applications in conjunction with solar parabolic concentrators. Yan et al. [58] proposed a new disk-shaped concentrator with a rotating array of homogeneous mirrors. The results showed that the concentrator maintained a good flux uniformity with a maximum concentration ratio of 2963. Sahu et al. [59] proposed a low-cost solar parabolic disk concentrator with an aperture of  $12.6 \text{ m}^2$  and dual-axis manual tracking. The results show that the concentrator offered in this work is more economical than other existing disk concentrators in the literature, costing Rs. 6877.00 per  $\text{m}^2$ . Liu et al. [60]

investigated the impact of tilt error on the tracking performance of a dish-type light gathering system, and Fig. 7 presents the corresponding results. The findings suggest that an azimuth axis tilt error leads to a decrease in the initial tracking position deviation within the horizontal or vertical plane, thereby compromising both the tracking performance and stability of the collector system compared to its original due east tracking position. To ensure simultaneous optimization of tracking performance and stability throughout the year-long operational it is recommended to maintain an azimuthal axis tangent angle  $\varphi_1 = 0^\circ$  (due south).

### Compound parabolic concentrators

Compound parabolic concentrators (CPCs) are capable of efficiently capturing both direct and diffuse solar radiation, rendering them an optimal choice for fixed-mounted non-imaging installations in CPV systems [61–63]. The inhomogeneous radiation introduced by CPC can be mitigated by integrating a homogenizer [64]. This homogenizer typically takes the form of a slender CPC extension, which ensures a more uniform distribution of radiation. Chandan et al. [61] studied the thermal and electrical performance of CPC-based low concentrating photovoltaic/thermal (LCPV/T) systems, both with and without homogenizers. They proposed integrating a homogenizer into an air-cooling system for LCPV/T. The findings demonstrate that the utilization of a long composite paraboloidal concentrator in LCPV/T can mitigate the adverse effects caused by nonuniform irradiation and enhance system efficiency compared to LCPV/T without a homogenizer. Furthermore,

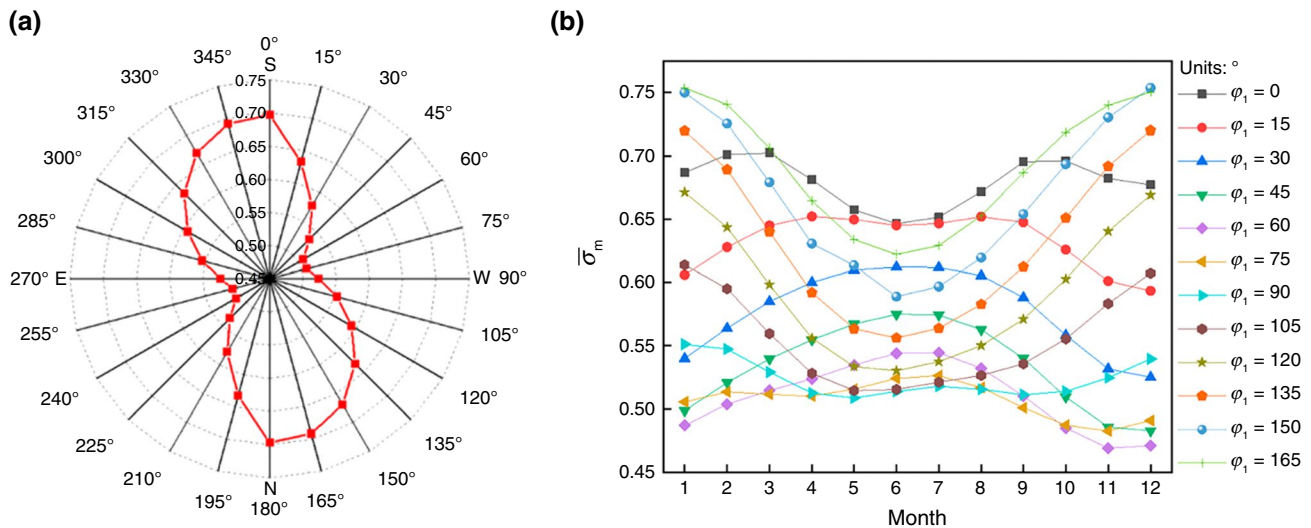


**Fig. 7** Variation of **a** annual mean effective tracking factor  $\bar{\sigma}_y$  and **b** monthly mean effective tracking factor  $\bar{\sigma}_m$  for the SDC system with different azimuth axis tilt errors [60]

employing a desiccant-based air-cooled system with two slender composite paraboloidal concentrator-based low-concentration photovoltaic thermal systems connected in series leads to a remarkable 50% improvement in performance factor. Zhang et al. [65] proposed a novel concentrator, the eliminating multiple reflections (EMR) CPC, which was investigated for its effects on the optical performance of concentrating photovoltaic/thermal (CPV/T) systems, temperature distribution of photovoltaic cells, and energy and exergy efficiency. The results demonstrate that as the truncation position decreases, the optical efficiency of the EMR concentrator increases, while there is a slight increase in irradiance and photovoltaic temperature nonuniformity initially followed by a decrease. From an energy and exergy perspective, the EMR concentrator with a height of 543 mm exhibits superior performance with electrical, thermal, and total energy efficiencies of 12.45%, 61.23%, and 73.68%, respectively.

It is imperative to conduct meticulous optimization and precise modeling predictions prior to practical implementation. Taking into consideration the impact of nonuniform radiation and temperature on the thermoelectric performance of the CPV/T system, Parthiban et al. [66] employed the Monte Carlo ray tracing (MCRT) technique to simulate the flux distribution of a CPC absorber under varying incidence angles. The study's results demonstrate the accuracy of the prediction results, with a maximum deviation of less than 3% in the solar cell temperature. The variation obtained when using nonuniform heat flow density is much smaller than that obtained when using average heat flow density. Zhang et al. [67] developed a two-dimensional

light-thermal-electric coupling model to predict the impact of photovoltaic temperature distribution on truncated CPC concentrating system performance. The findings demonstrate that, with an increasing concentration ratio, the irradiance and photovoltaic temperature inhomogeneity at the lowest eliminating multiple reflections (LEMUR) exhibit a faster increase compared to those at the highest eliminating multiple reflections (HEMR). Consequently, as the concentration ratio increases, both filling factor and electrical efficiency experience a more pronounced decline at LEMUR than at HEMUR concentration.

### Trough concentrators

Meng et al. [68] proposed a novel trough-free secondary solar concentrator (TFSC), comprising of a primary trough concentrator and a secondary free-form reflector, to enhance the thermal cycling performance of CPV module application. Otanicar et al. [69] designed a secondary light concentrator by utilizing the existing primary light concentrator of a parabolic trough solar thermal plant, as depicted in Fig. 8a. Experimental results demonstrate that the secondary light concentrator achieves a maximum measured cell efficiency of 25.4%, as shown in Fig. 8b. Ullah et al. [70] studied an optical model of a CPV system consisting of a primary parabolic trough and a secondary non-imaging reflector. The findings demonstrate that the proposed concentration level compared to the conventional slotted concentrator system, enabling it to achieve a geometric concentration of 285. Iqbal et al. [71] proposed a slotted non-imaging CPV system, comprising of a primary concentrator in the form of a parabolic slot and a secondary concentrator in the form of a

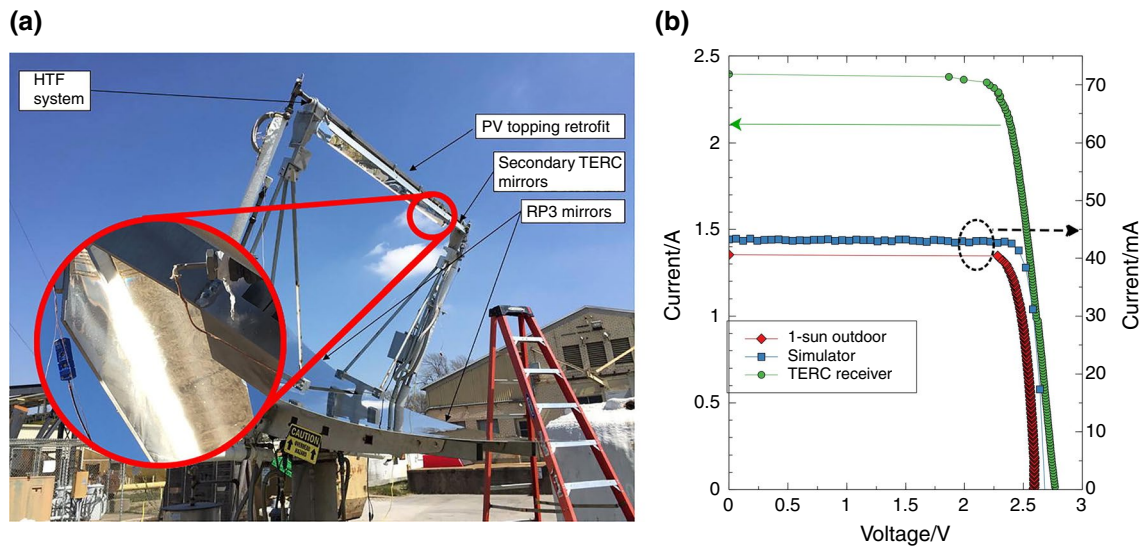


**Fig. 8** **a** Schematic diagram of the modified secondary concentrator; **b** The  $I$ - $V$  curve of the Cell 31 varies with the solar simulator (right vertical axis), the outdoor single-sun test (right vertical axis), and the centralized Tailored Edge Ray Collector Concentrating Photovoltaic receiver [69]

non-imaging reflective slot. The CPC achieves an impressive concentration ratio of  $622\times$  with an optical efficiency reaching 79%. Qu et al. [72] developed a spectroscopic parabolic trough concentrator that effectively divides and concentrates incident solar radiation. Their study demonstrates that by utilizing monocrystalline Si photovoltaic, it is possible to achieve a solar power efficiency of approximately 31.8%. This represents an increase in efficiency by 15.3% and 6.3%, respectively, when compared to single systems alone.

The performance of parabolic trough collectors is significantly influenced by the thickness of the concentrator. Chan et al. [73] conducted a comprehensive analysis, including theoretical calculations, simulations, and experimental validation, to investigate the impact of mirror refraction on the concentration at various concentrator thicknesses. The findings reveal that a fivefold increase in concentrator thickness leads to a proportional increase in focal plane width and a fivefold decrease in maximum flux density at the focal plane. Additionally, there is a marginal reduction of 0.24% in optical efficiency. Gong et al. [74] proposed a large-aperture parabolic slot focusing system consisting of a new planar secondary reflector and an improved absorber tube. Analysis of the system's optical, thermal, and thermodynamic models through the study shows that using a large-aperture parabolic slot concentrator can reduce costs and improve cycle efficiency. Rehman et al. [75] proposed a method to optimize the shape of the concentrator, aiming for high flux uniformity while maintaining the same geometrical characteristics as the parabolic trough concentrator (PTC). The optimization results demonstrated that by achieving a concentration ratio of 8.96 and a solar flux distribution uniformity factor ( $\mu$ ) of 0.068, it was possible to obtain a concentrator with a  $C$  value

close to that of PTC but significantly improved  $\mu = 0.752$ , resulting in an approximately tenfold enhancement.

The V-trough is a variant of the trough concentrator design. Alqurashi et al. [76] employed a ray-tracing technique based on the finite element method to investigate the performance of a non-tilted CPV system with V-trough concentrator, in absence of a tracking system. The findings demonstrate that the utilization of V-trough concentrator can enhance the radiance of photovoltaic panels. To mitigate system costs and minimize energy losses resulting from the angle of incidence, Río et al. [77] proposed a two-dimensional cone-textured anti-reflective coating (ARC) for a V-trough photovoltaic concentrator. To mitigate the impact of temperature rise on CPV system efficiency, Alqurashi et al. [78] employed COMSOL Multiphysics software to investigate the thermal profile of a V-trough solar concentrator. By utilizing air cooling as the medium, their study revealed that reducing the reflector size resulted in partial coverage of the photovoltaic surface by solar radiation, thereby diminishing the temperature gradient without completely eliminating it. Alnajideen et al. [79] proposed an innovative design for a V-trough solar concentrator (OVSC) by arranging two conventional V-trough concentrators in a crosswise manner to enhance the concentration ratio. Their study findings demonstrate that OVSC achieves a 40–60% higher concentration ratio compared to conventional V-trough solar concentrators (CVSC), while also offering additional advantages. Moreover, OVSC exhibits significant cost reduction potential in comparison with CVSC.



## Other concentrators

To mitigate the detrimental impacts of nonuniform radiation, temperature fluctuations, and shadowing on the concentrated photovoltaic (CPV) system, Narasimman et al. [80] proposed a linear ridge concentrator photovoltaic system incorporating 1-Sun and 2-Sun concentrations as a viable solution to address the aforementioned challenges. The results demonstrate that the output power gains for 1-Sun, 2-Sun, 1-Sun with tilt, and 2-Sun with tilt are increased by 11.5%, 24.3%, 19.2%, and 48.89%, respectively, compared to the reference photovoltaic module. Furthermore, the efficiency gains for these configurations (i.e., 1-Sun, 2-Sun, 1-Sun with SBA-15 and 2-Sun with SBA-15) are found to be enhanced by approximately 6%, 7.4%, 12.1% and 16.2%, respectively, in comparison to the reference module.

Ustaoglu et al. [81] proposed a new photovoltaic–thermal system (CHCT-PVT) consisting of a composite hyperbolic concentrator-horn type concentrator. The results show that the CHC-CPV system requires only half the size of a v-tank or CPC system to achieve the same electrical power as such a system at the same concentration. To address the challenges of complex manufacturing, assembly, and low efficiency associated with planar concentrators, Wei et al. [82] proposed a side absorption concentrating photovoltaic (SCPV) system that utilizes a single concentrating element. This design offers several advantages including a compact structure, feasible manufacturing and assembly processes, and high efficiency. Wang et al. [83] proposed a CPV system that utilizes a multi-segment plate concentrator, as depicted in Fig. 9b. The results demonstrate that the concentrator not only exhibits high uniformity of light concentration but also demonstrates superior photoelectric conversion efficiency compared to the CPV system with a parabolic slot concentrator. Furthermore, its geometric concentration ratio

increases as the solar cell mounting height rises. As shown in Fig. 9b, under normal solar tracking conditions, the relative optical efficiency of CPV systems can reach 0.8 or even higher.

Xu et al. [84] proposed a lens-based, non-tracking photovoltaic system for low-concentration applications, as depicted in Fig. 10a. In contrast to the composite parabolic concentrator, this novel design offers an expanded light reception range and allows for adjustment of the installation angle only four times per year. It effectively and uniformly concentrates sunlight onto the cell surface for 5 h daily, achieving an average optical efficiency of 0.77 (Fig. 10b) and a heat flow distribution uniformity of 0.75 (Fig. 10c). Furthermore, it exhibits a maximum temperature difference on the cell surface of only 18.93 °C while maintaining a temperature distribution uniformity above 0.89 °C, as depicted in Fig. 10d. Kolaroudi et al. [85] proposed using mirrors for LCPV systems to maximize the output power of photovoltaic systems, and four experimental setups are depicted in Fig. 11a. By observing Fig. 11a and c, it can be seen that the implementation of a cooling system on the panel surface, in conjunction with perpendicular placement of four-sided reflector mirrors, results in a threefold increase in output power compared to non-concentrator systems. Furthermore, the utilization of concentrators leads to an average output power enhancement by 2.84 times when compared to systems without concentrators. Ayane et al. [86] studied a microphotovoltaic concentrating system with a geometric concentration ratio of 100 times consisting of a plano-convex lens as the primary optical element, a spherical lens as the second optical element, and a solar cell, as shown in Fig. 12a. The research results are shown in Fig. 12b, and the system's optical efficiency is 92.13% at a simulated reception angle of 1.1°.

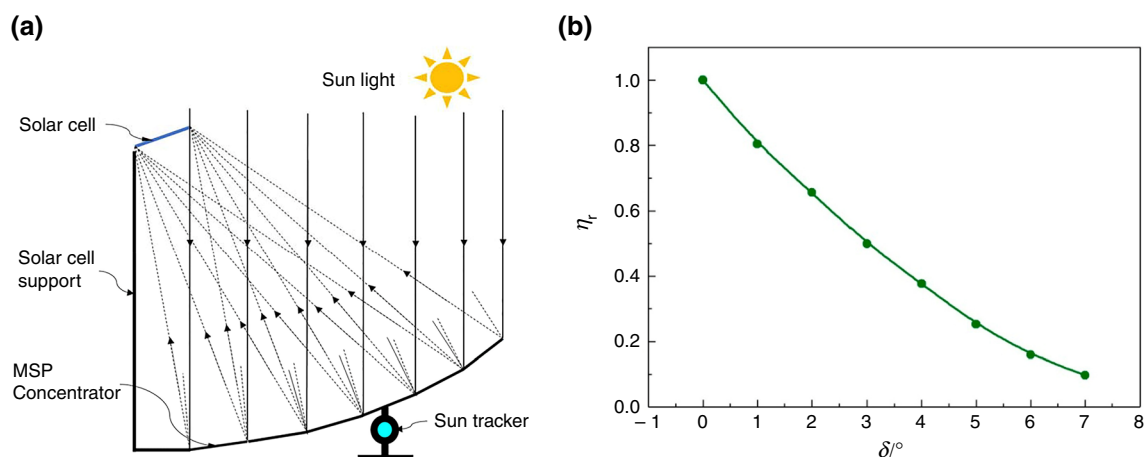


**Fig. 9** **a** Schematic diagram of the multi-segment plate concentrator; **b** The tracking error effect on the relative optical efficiency [83]

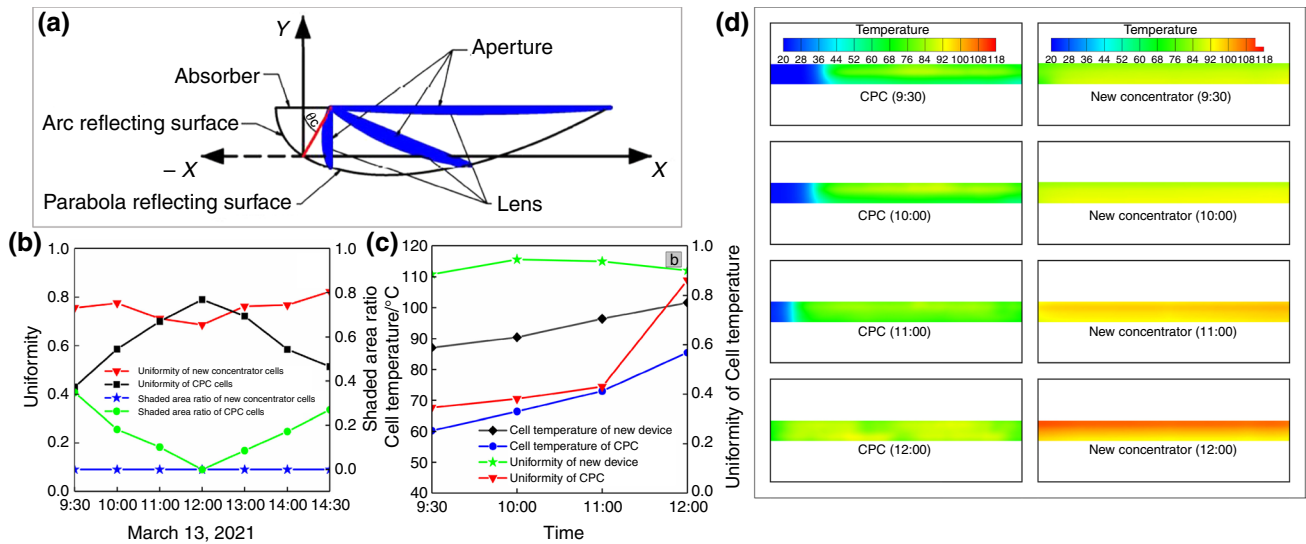


**Fig. 10** **a** Schematic representation of the geometric structure of the novel concentrator; **b** Evaluation of shadow area proportion on the cell surface and uniformity analysis of heat flux distribution at different time intervals for the concentrator; **c** Assessment of average tem-

perature on the solar cell surface and temporal variations in temperature uniformity; **d** Comparative analysis of temperature distribution on the cell surface between compound parabolic concentrators and new concentrator at various time points [84]

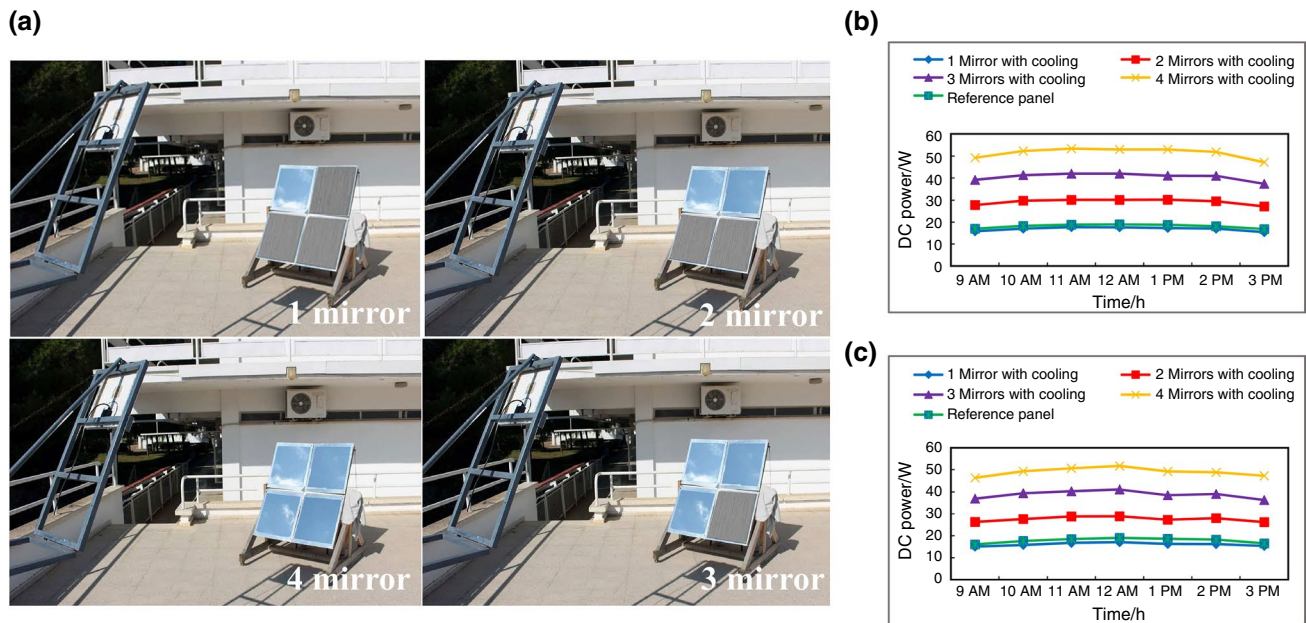


**Fig. 11** **a** Diagram of experimental research objects; The DC power generation for reference panel and low concentrating photovoltaic system with cooling by 1–4 mirrors in summer average **(b)** and typical day **(c)** in September 2020 under the circumstances of Famagusta, Cyprus [85]

The luminescent solar concentrator (LSC) is a light absorber that utilizes cost-effective polymeric materials with optical windows a substitute for conventional photovoltaic modules, thereby effectively reducing the levelized cost of energy (LCOE) associated with photovoltaic power [87]. Delgado-Sanchez et al. [88] investigated the role of tunable photoluminescent optical layers in LSCs. The findings

demonstrate that the tunable photoluminescent optical layer can be extended to accommodate six dyes in randomly oriented configurations, thereby showcasing its inherent advantage of tunability and resulting in a notable 16.2% increase in LSC optical efficiency. Nie et al. [89] proposed a smart LSC for BIPV windows, which consists of a waveguide and a thermochromic hydrogel film doped with the

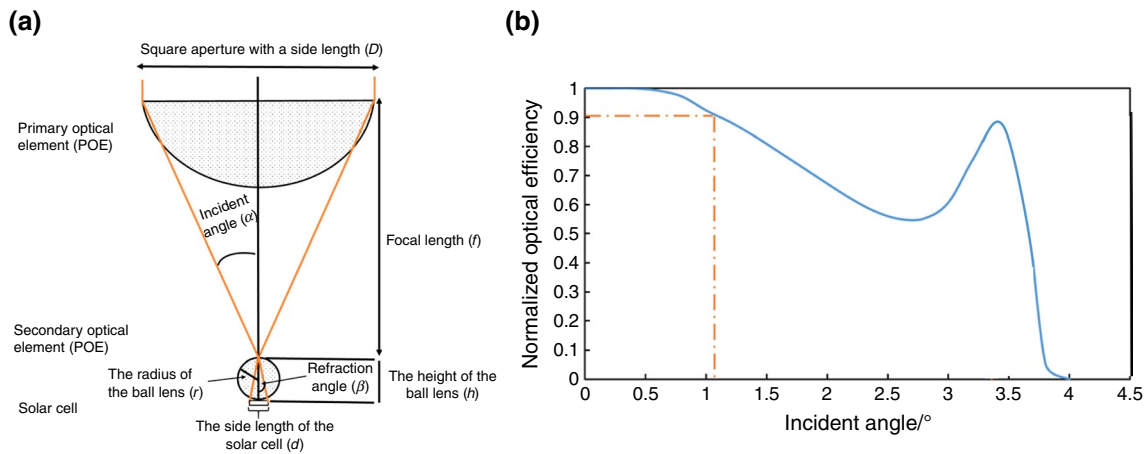
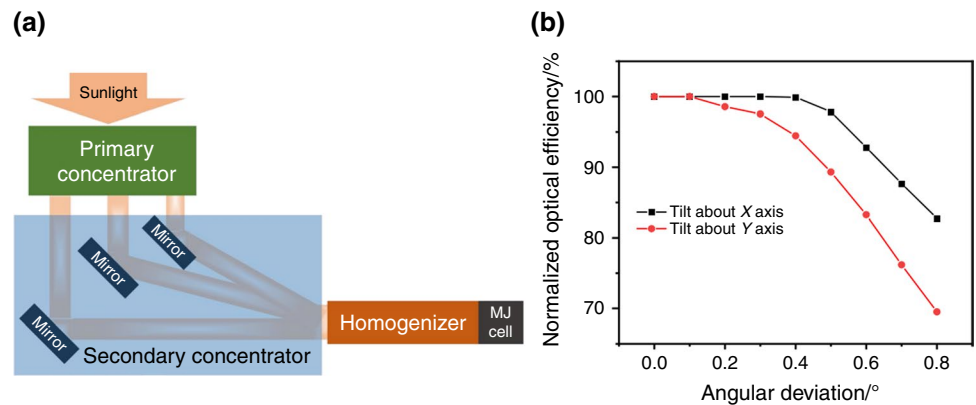


**Fig. 12** **a** Schematic diagram of the geometry of the miniature concentrator; **b** Optical efficiency of the micro concentrator versus incident angle [86]

**Fig. 13** **a** Schematic diagram of concentrating photovoltaic system; **b** Normalized optical efficiencies of high concentrating photovoltaics system under various incidence angles along x-axis and y-axis [91]



organic dye Lumogen F Red-305 (BASF). By simulating a 100 mm × 100 mm × 3 mm smart LSC with a bottom solar cell measuring 100 mm × 10 mm, an optically effective concentration range of 1.23–1.31 was achieved, resulting in an experimental power gain of up to 1.26 over the bare solar cell. Qu et al. [90] proposed and designed a spectroscopic concentrator, which demonstrated an absolute increase in the conversion efficiency of solar energy to electricity and fuel by > 5% compared to photovoltaic and solar thermal power alone. To enhance the concentration ratio of HCPV systems, Vu et al. [91] proposed a solar concentrator with a concentration ratio exceeding 1000×, as depicted in Fig. 13a. The system comprises a primary double-lens concentrator, a secondary concentrator, and a homogenizer for achieving high concentration ratios. The research results are shown in Fig. 13b, and the efficiency of the CPV system utilizing such concentrators can attain up to 75%.

To optimize solar energy collection for the purpose of renewable energy generation and facilitate light-harvesting functionalities, Xuan et al. [92] devised a two-dimensional static concentrator featuring an uncoated lower section near

the base area to establish a “daylighting window” (CPVD), as illustrated in Fig. 14a. The study findings revealed that the average daily transmittance of CPVD was measured at 8.73% under clear-sky conditions (as shown in Fig. 14b), while a lower light transmission rate of 7.11% was observed during cloudy conditions (as Fig. 14c). Lv et al. [62] proposed a design methodology for an indoor lighting system that utilizes planar concentrators as light-harvesting modules, enabling the achievement of illuminance levels above 500 lx and meeting commercial lighting requirements. In the field of agricultural utilization, Vu et al. [93] proposed a solar spectral splitting CPV system designed for dual land use, comprising a free-form lens array and planar waveguides. The findings of their study demonstrate that this system can achieve a light efficiency exceeding 82.1% for blue and red light transmission, over 94.5% for diffuse sunlight in agriculture applications, and more than 81.5% for planar waveguide light efficiency in power generation at a concentration level of 200 times.

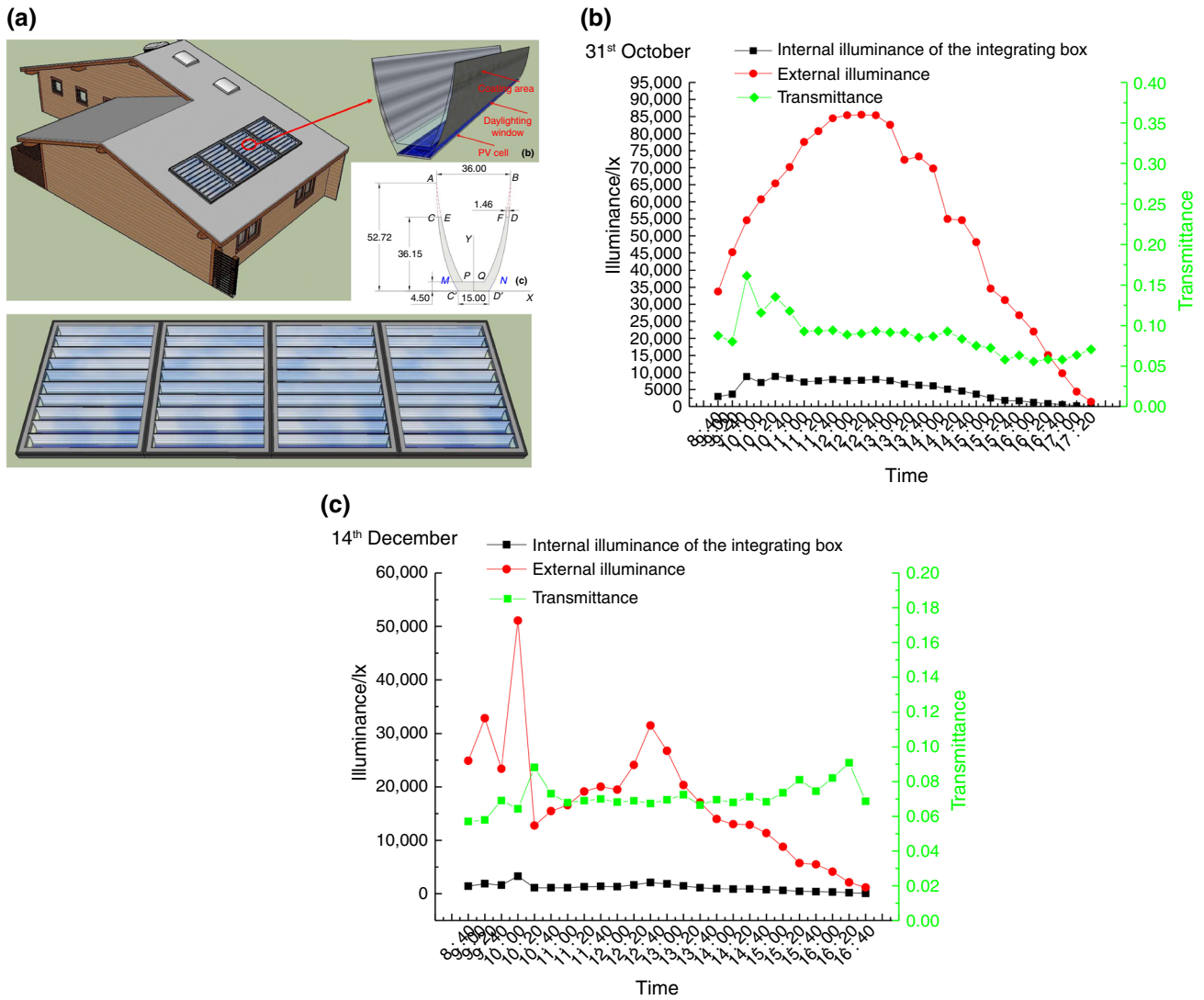


**Fig. 14** **a** Schematic diagram of the “daylighting window” (CPVD); **b** Instantaneous integral box illuminance, external illuminance, and transmittance of the system under direct solar radiation on October

31; **c** Instantaneous integral box illuminance, external illuminance, and transmittance of the system under diffuse solar radiation on December 14 [92]

### Solar tracker

The fixed tilt of the CPV panel restricts its ability to track the sun’s movement, resembling a static structure rather than a dynamic “sunflower” [94]. Consequently, conventional CPV systems suffer from the drawback of incomplete utilization and nonuniform distribution of solar radiation. To address this issue effectively, solar trackers have been introduced as an efficient means to enhance photovoltaic system efficiency [95, 96]. The introduction of single-axis and dual-axis solar trackers enables CPV systems to achieve uniform radiation distribution and optimize solar energy utilization [97, 98]. Previous studies have indicated that single-axis solar tracking systems can enhance the power output of photovoltaic modules by approximately 20% compared to

fixed-axis configurations [99]. In contrast, dual-axis solar trackers can increase the power output of photovoltaic modules by around 33%.

### Single axis

The single-axis ST system is considered the most cost-effective option for power generation when compared to the dual-axis solar tracker [100]. However, it is more susceptible to environmental and climatic factors, which may result in additional maintenance expenses. Taking into consideration the influence of wind loads, Martínez-García et al. [101] investigated the impact of panel inertia and aspect ratio on the initiation of torsional runout. The findings indicate that while the tilt angle affects the critical deceleration speed for

Mercedes vehicles, it is predominantly unaffected by key structural parameters such as torsional stiffness, inertia, and spreading ratio. Considering the effect of parameters such as wind direction and module inclination on the development of wind load disturbance in single-axis solar trackers, Valentín et al. [102] conducted an investigation on the torsional vibration failure of single-axis solar trackers. The findings from this study revealed that the loss was attributed to high-speed winds and the resulting torsional fly-by phenomenon when the solar tracker tilted to  $0^\circ$ . Ma et al. [103] conducted wind tunnel tests to measure the pressure on single-axis solar trackers and tracker arrays using rigid models, aiming to investigate the impact of tilt angle and wind direction on their aerodynamic characteristics. The study findings demonstrate that the interference effect becomes increasingly significant with an increase in tilt angle. Wind-excited vibrations have a greater impact on the solar modules located at the rear end of the solar tracker array compared to those at the front. The influence uneven distribution of wind loads along the length of the solar tracker. Therefore, when designing solar trackers, it is crucial to consider how wind direction enhances wind load on the edge area of the solar array.

Revisiting the impact of climate on tracker performance, Kuttybay et al. [104] conducted an investigation into the operational efficiency of single-axis solar trackers and stationary photovoltaic installations across diverse weather conditions. The study findings demonstrate that the schedule-based solar tracking system exhibits a 4.2% higher efficiency compared to the LDR solar tracker under diverse weather conditions. Moreover, the tracker outperforms a fixed solar panel set at the optimal tilt angle by an impressive margin of 57.4%. Considering the orientation sensitivity of solar tracker, Gómez-Uceda et al. [105] investigated the impact of terrain orientation on uniaxial solar tracker systems. The findings suggest that, for non-south-facing land, aligning the azimuth of the rotation axis of the solar

tracker with the same orientation as that of the land can optimize energy production. Chu et al. [106] conducted a series of wind tunnel experiments on a rooftop-mounted solar tracking system. The findings demonstrate that the wind's angle of attack on the tracker is a crucial parameter for assessing its wind load, irrespective of wind direction and azimuth. Moreover, an increase in base height and tilt angle leads to an elevation in net pressure exerted on the tracker. Campos et al. [107] proposed a novel model based on angular deviation control in single-axis structures, aiming to minimize the manufacturing and maintenance costs of single-axis ST systems. The analysis results demonstrate that this optimization approach for single-axis ST can effectively reduce panel displacements, thereby mitigating mechanical wear and tear as well as energy consumption.

### Dual axis

Dual-axis solar tracker, in comparison to the single-axis solar tracker, offers 2 degrees of freedom enabling it to track the sun both vertically and horizontally, thereby achieving optimal efficiency [108]. Wu et al. [109] proposed an enhanced dual-axis solar tracker to address the challenges of low solar incidence angle and manual orientation/elevation calibration, thereby enhancing the performance of solar energy collection. The study findings demonstrated that this solar tracker achieved automatic alignment with the sun, ensuring robustness, convenience, and reliability across different geographic locations and photovoltaic panel constraints. To enhance the precision of solar energy tracking by the dual-axis solar tracker and optimize energy harvesting for the HCPV system, Satué et al. [110] proposed an automatic calibration algorithm. The algorithm presented herein enables a greater tolerance during the installation process by employing error estimation techniques, thereby obviating the need for extensive time investment in error minimization. Dahlioui et al. [111] proposed an integrated cleaning

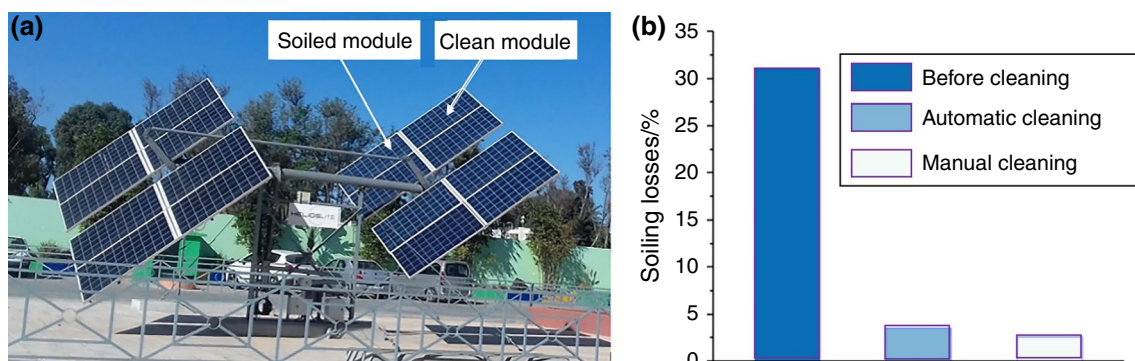


**Fig. 15** **a** Diagram of a dual-axis concentrating photovoltaic system with automatic cleaning function; **b** The resulting graph of soiling losses recovery by manual and automatic cleaning [111]

system that combines a two-axis solar tracker system with an automated cleaning mechanism, as depicted in Fig. 15a. The research results are shown in Fig. 15b, and within arid regions, the efficacy of automatic cleaning was comparable to manual cleaning, with only a marginal difference of 0.95 pp and an energy increment of 11.5%.

While the majority of research has primarily focused on solar tracking systems to enhance the incident solar radiation on photovoltaic panels, limited attention has been given to manually adjusting the tilt mechanism. Consequently, Gönül et al. [112] conducted a techno-economic comparison of solar tracking systems (including fixed-tilt, single-axis east–west (SA-EWT), single-axis north–south (SA-SNT), and dual-axis (DAT)) equipped with manually adjustable tilt mechanisms. The analysis revealed that implementing monthly manual adjustments to the tilt emerged as the most viable solution, resulting in a reduction in the payback period for the fixed tilt system by approximately 8 months to 9.6–12.6 years and an enhancement in power generation by 3.6–5%. Badr et al. [113] proposed a two-axis elliptical solar tracker, as shown in Fig. 16a. The study results indicate that the measurement error of the solar tracker is not affected by dusty or cloudy weather. Additionally, according to Fig. 16b and Fig. 16c, the maximum temperature recorded for the solar cell was approximately 42 °C. The electrical power obtained from a solar cell area of 1.012 cm<sup>2</sup> was 1.08 W.

To address the challenges of photovoltaic power generation, Hua et al. [114] conducted an analysis on various solar trackers. The findings indicate that the horizontal axis tracker, in conjunction with its bifacial module, complements other solar trackers. Hammoumi et al. [115] proposed a cost-effective and simplified design of an active dual-axis solar tracker (DAST), which offers the advantages of minimal components and low expenses. The research findings demonstrate that the intelligent DAST system yields an energy increase of 36.26% compared to fixed panels.

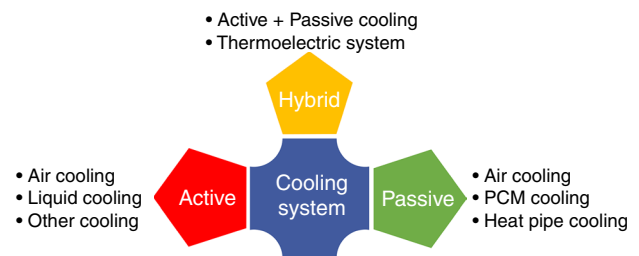
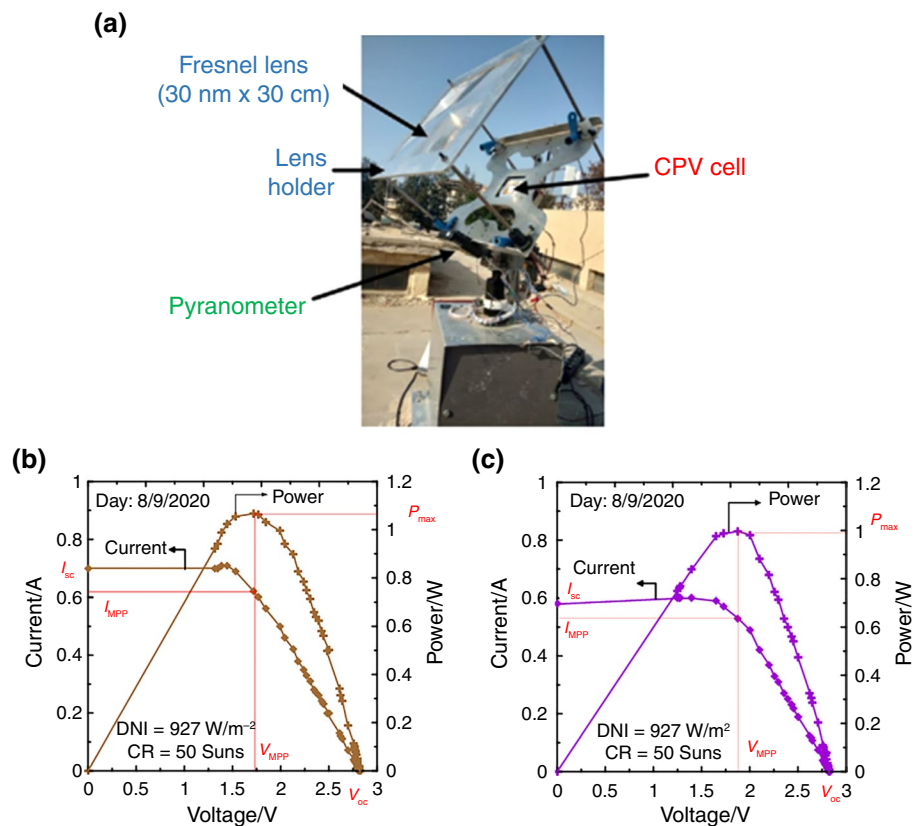


Fig. 17 The thermal management approach for concentrating photovoltaic systems

Fig. 16 a Diagram of the experimental setup of a concentrating photovoltaic system based on a two-axis elliptical solar tracker; Variation of the IV and photovoltaic curves for the concentrator photovoltaic cell at concentration ratio of 50 Sun at b DNI=982 W m<sup>-2</sup>, and (c) DNI=927 W m<sup>-2</sup> [113]



## Cooling systems

The high operating temperature on the surface of photovoltaic cells poses another challenge for CPV systems, as it can adversely impact the system [116, 117]. The effective thermal management is crucial for the development and commercialization of CPV systems [118]. Figure 17 summarizes several thermal management approaches taken by CPV systems. It is classified into active, passive, and hybrid cooling according to the presence or absence of an external power source. An efficient cooling system should be capable of reducing the overall temperature while maintaining a uniform distribution [119–121]. Hence, the choice of cooling medium plays a pivotal role in enhancing the efficiency of CPV systems. In this section, we will provide a comprehensive review of the research advancements and limitations pertaining to cooling systems for CPV applications, categorized into three types: active cooling, passive cooling, and hybrid cooling systems.

### Active cooling system

Active cooling systems increase the media's cooling capacity by varying the media's flow through a pump control system or an electronic control valve [34, 122]. Active cooling systems can provide an excellent cooling source for HCPV systems [123, 124]. The heat collected through the dynamic cooling system can be used extensively for cryogenic applications. However, increasing the light flow rate increases the electrical consumption of the pump. Therefore, it is necessary to determine an appropriate mass flow rate to maximize electrical and thermal efficiency. This section will review the research progress and status of typical passive cooling technologies in the last 5 years.

#### Air cooling

Air cooling has been the predominant active cooling system over the past 2 decades, and its development has reached a relatively advanced stage [122]. However, its growth is constrained by environmental limitations. Therefore, addressing these limitations necessitates synergistic integration with other cooling methods. This aspect will be comprehensively discussed in the subsequent section.

#### Liquid cooling

The active water cooling technique is widely adopted due to its straightforward design, exceptional heat dissipation capability, and effortless operation, making it the simplest and most cost-effective among all cooling methods [125]. Goma et al. [126] conducted an evaluation on the

performance of planar photovoltaic/thermal and CPV/T systems utilizing water as the active cooling working fluid. The study findings demonstrate that a maximum electrical energy output of 170 W and a total thermal energy output of 580 W can be achieved at a concentration ratio of 3 and a cooling water flow rate of  $1 \text{ kg min}^{-1}$ . The direct contact liquid film cooling (DCFC) is a type of active water cooling technology that utilizes deionized water to extract heat from the rear side of solar cells. Wang et al. [127] investigated the impact of employing the DCFC technique on the performance of tilted high-concentration photovoltaic cells. Under experimental conditions including solar cell tilt angles ranging from  $0^\circ$  to  $75^\circ$ , inlet flow rates between 100 and  $300 \text{ L h}^{-1}$ , and inlet temperatures varying from 30 to  $75^\circ\text{C}$ , an optimal angle for liquid film cooling was determined as  $20^\circ$ . Moreover, in practical applications, photovoltaic panels are susceptible to contamination from pollutants such as dust and dirt. To mitigate the impact of surface contamination on CPV panel efficiency, Acar et al. [128] conducted experiments on an active system designed for cleaning and cooling photovoltaic modules. The study findings demonstrate that the system facilitates both automated cleaning and cooling processes. The application of the cleaning-cooling process results in a temperature reduction of  $17^\circ\text{C}$  in the photovoltaic module compared to those without this process. Furthermore, the proposed design leads to a remarkable enhancement of 40% in power output for the photovoltaic modules. The flow of coolant consumes pumping power, resulting in a decrease in net power output. Therefore, it is imperative to determine the optimal operating conditions for systems employing active water cooling. Sharma et al. [129] investigated the optimum concentration ratio for an advection-cooled concentrated photovoltaic (ACCPV) method through numerical analysis using COMSOL Multiphysics software. The findings revealed that the optimal concentrations for m-Si, p-Si, a-Si, CIGS, and CdTe cells were 7, 9, 16, 9, and 20, respectively. Correspondingly, the respective water mass flow rates were determined as  $0.055 \text{ kg s}^{-1}$ ,  $0.111 \text{ kg s}^{-1}$ ,  $0.098 \text{ kg s}^{-1}$ ,  $0.103 \text{ kg s}^{-1}$ , and  $0.161 \text{ kg s}^{-1}$ .

Additionally, microchannel cooling has been shown to enhance water cooling [130]. In recent years, microchannel flow boiling has garnered increasing attention as a highly promising solution for the propulsion cooling of high-throughput devices. However, the fluctuations and inhomogeneities of CPV heat flow pose a challenge to microchannel boiling for cooling CPV [131]. Yu et al. [132] studied the transient flow and phase transition phenomena in deionized water microchannels by numerical simulation of flow boiling. The impact of sudden increases in heat flow density on the two-phase flow pattern of flow boiling was investigated. The findings demonstrate that higher additional heat flux leads to diverse evolutions in the flow

pattern, with more significant sudden heat flux increases resulting in severe alterations. Wu et al. [133] investigated the electrical and thermal behavior of a multi-stage channel active cooling heat sink for CPV solar cells under indoor (248cr) and outdoor (500× and 900× concentration ratio) conditions. The study findings demonstrate that the number of channels exerts a significant impact on the heat sink performance. Increasing the inlet water flow rate or reducing the inlet water temperature substantially lowers the maximum temperature of the CPV solar cell, leading to enhanced output power. The electrical efficiency of this heat sink-integrated CPV cell reaches approximately 30%, while its cogeneration efficiency achieves around 88%. Varghese et al. [134] proposed a MEMS heat sink with a serpentine microchannel made of Si. The results demonstrate that an increase in Reynolds number leads to a proportional rise in pump power and a corresponding decrease in thermal resistance, irrespective of the MEMS heat sink geometry. Furthermore, the characteristics of the serpentine microchannel MEMS heat sink also exhibit independence from the spotting ratio.

However, liquid cooling systems are constrained by nonuniform temperature distribution and temperature elevation along the flow [135]. A spray cooling system can overcome the limitation of variable temperature while also achieving efficient cooling performance and water conservation. Jowkar et al. [130] first investigated the impact of spray cooling methods on commercial joule cells, as depicted in Fig. 18a. The study demonstrated that spray cooling effectively reduced the cell temperature below the permissible operating range of 353 K, as depicted in Fig. 18b. Furthermore, an increase in the nozzle-to-surface distance resulted in a maximum cell temperature exceeding the allowable range by 2–14% at various concentration ratios. Ansari et al. [135] proposed a modified cooling duct design featuring an

isothermal heat sink with a cylindrical pin microstructure for dense concentrating photovoltaic systems. The results indicate that in the best case, the maximum temperature variation of the UHV heatsink is only 1.56 K, which is 84.1% lower than its original value (9.82 K). There is a reduction in pumping power by 33.1%. Han et al. [28] proposed a vapor chamber cooling method for a CPV system based on a multi-segment mirror concentrator. The study's results showed that the temperature of the CPV cell with a vapor chamber was 17.5 K lower than that without, thus improving the electrical performance of the system. The steam chamber cooling system can maintain the maximum instantaneous temperature of the CPV cell at 323.8 K under 30 solar concentrations, with minimum and average electrical efficiencies of 13.9% and 14.4%, respectively, throughout the day.

Conventional heat transfer fluids, such as water and oil, exhibit limitations in terms of capacity and heat transfer rate [136]. Nanofluids, composed of nanoparticles with particle diameters below 100 nm dispersed in essential fluids like water and oil, represent a novel class of heat transfer fluids [137, 138]. They possess the ability to efficiently absorb solar energy, convert it into heat, and demonstrate exceptional thermophysical properties including thermal conductivity and heat transfer efficiency [139, 140]. Consequently, nanofluids offer a promising solution to overcome the constraints associated with conventional heat transfer fluids. Elminshawy et al. [141] investigated an active cooling system for CPV modules using two different flow rates of pure water and water-based nanofluids as coolants. The preparation procedure of Al<sub>2</sub>O<sub>3</sub> nanofluid is shown in Fig. 19a. The experimental results show that the electrical output, electrical efficiency, and thermal efficiency of Al<sub>2</sub>O<sub>3</sub> nanofluid-based CPV with a concentration of 0.7% were enhanced by 10.40%, 10.24%, and 35.79%, respectively, compared to those obtained with pure water, as depicted in Fig. 19b.

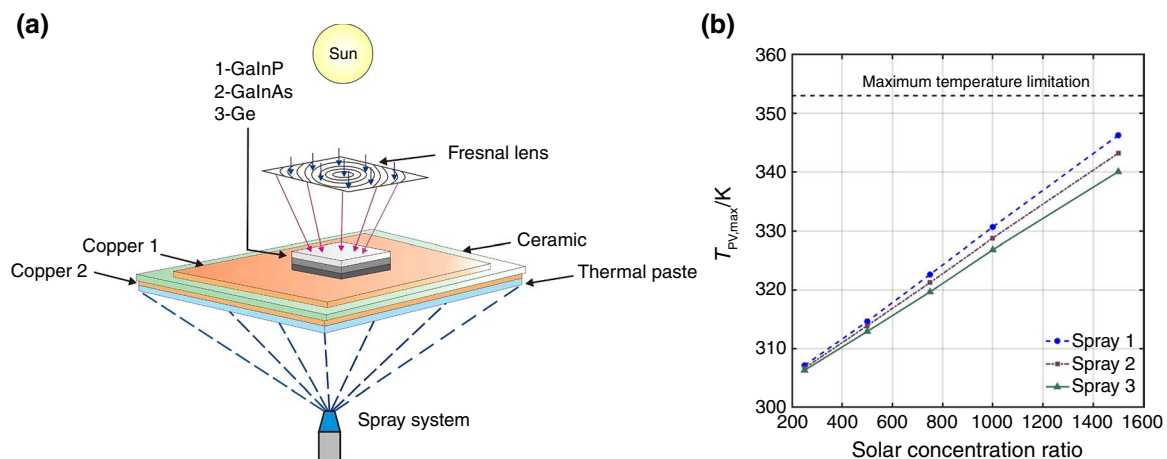


**Fig. 18** **a** High concentrating photovoltaic assembly integrated with spray cooling system; **b** Variations of maximum cell temperature with solar concentration ratio [130]



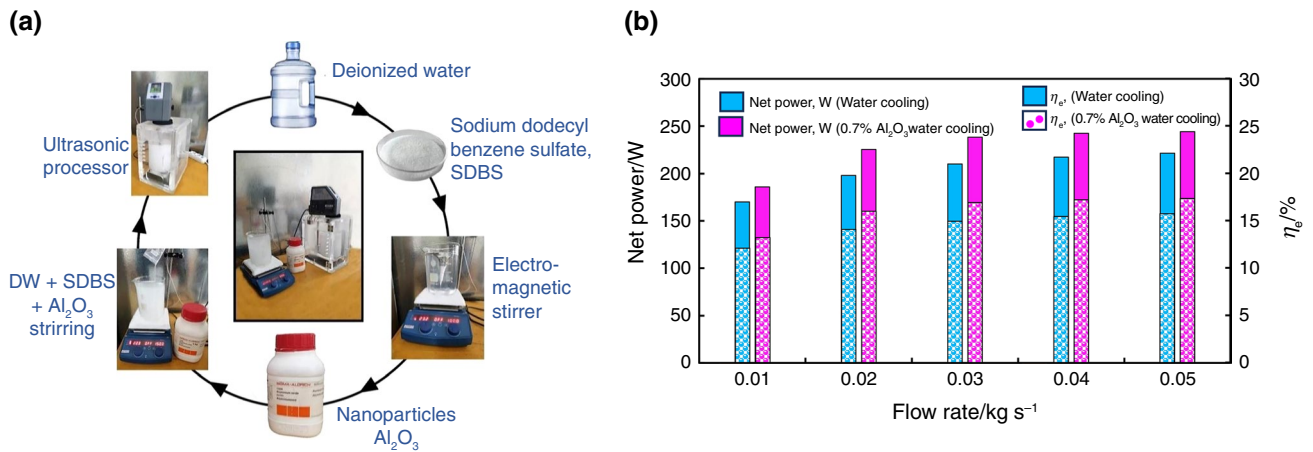


**Fig. 19** a Procedure of Al<sub>2</sub>O<sub>3</sub>/water nanofluid preparation; b Net electrical power and the electrical efficiency of concentrating photovoltaic module versus nanofluid mass flow rates [141]

Rubbi et al. [142] investigated the effect of two-dimensional MXene (Ti<sub>3</sub>C<sub>2</sub>), Therminol55 oil-based mono- and hybrid nanofluids on the performance of CPV/T systems. The study results indicate that the nanofluid exhibits an excellent cooling effect on the photovoltaic modules in the system, resulting in temperature reductions of 25 °C and 24 °C for single and mixed nanofluids, respectively. Salem et al. [143] investigated the cooling process required for implementing a CPV system using Al<sub>2</sub>O<sub>3</sub>/H<sub>2</sub>O as a nanofluid. The results indicate that increasing the particle concentration or reducing the particle size can significantly enhance the heat transfer coefficient. Conversely, nanofluids lead to a substantial increase in pumping power, particularly when there is greater attention given to reducing particle size.

**Other cooling**

In addition to the typical types of active cooling systems mentioned above, researchers have investigated several new potential active cooling systems in CPV systems. Elminshawy et al. [144] assessed the impact of utilizing a buried water heat exchanger (BWHE) as an active cooling system

on the performance of a V-trough photovoltaic concentrator. The BWHE cooling system successfully reduced the panel surface temperature from 72.5 °C to 47.2 °C, 45.5 °C, 41.8 °C, and 39.3 °C at water cooling flows of 0.01 kg s<sup>-1</sup>, 0.02 kg s<sup>-1</sup>, 0.03 kg s<sup>-1</sup>, and 0.04 kg s<sup>-1</sup>, respectively. At these water cooling flow rates (0.01 kg s<sup>-1</sup>, 0.02 kg s<sup>-1</sup>, 0.03 kg s<sup>-1</sup>, and 0.04 kg s<sup>-1</sup>), the peak electrical power generation (GEP) increased by 18.6%, 20.9%, 23.5%, and 28.3%, respectively, compared to the uncooled panels. The electrical and thermal efficiencies increased with the increase in cooling water flow. Ji et al. [145] proposed an active cooling method that utilizes silicone oil as the cooling medium, which allows the silicone oil to flow directly through both sides of the cell without obstructing light transmission, as shown in Fig. 20a. The results, as depicted in Fig. 20b, demonstrate that heat transfer fluids containing silicone oil can effectively maintain solar cells within a safe operating temperature range and facilitate the removal of excess heat. Tan et al. [119] developed a metal foam heat sink with a functional gradient for CPV systems and investigated the effect of porosity and pore density on the flow field and thermal performance of aluminum foam heat sinks. The

**Fig. 20** a Schematic diagram of the method of collecting waste heat from both sides of the photovoltaic cell by silicone oil; b The real-time measured temperatures throughout outdoor testing of a transmissive direct fluid-cooled concentrating photovoltaic module [145]

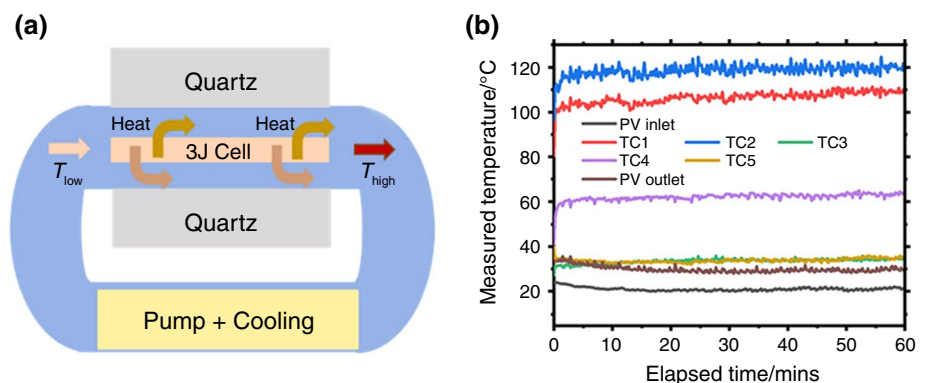
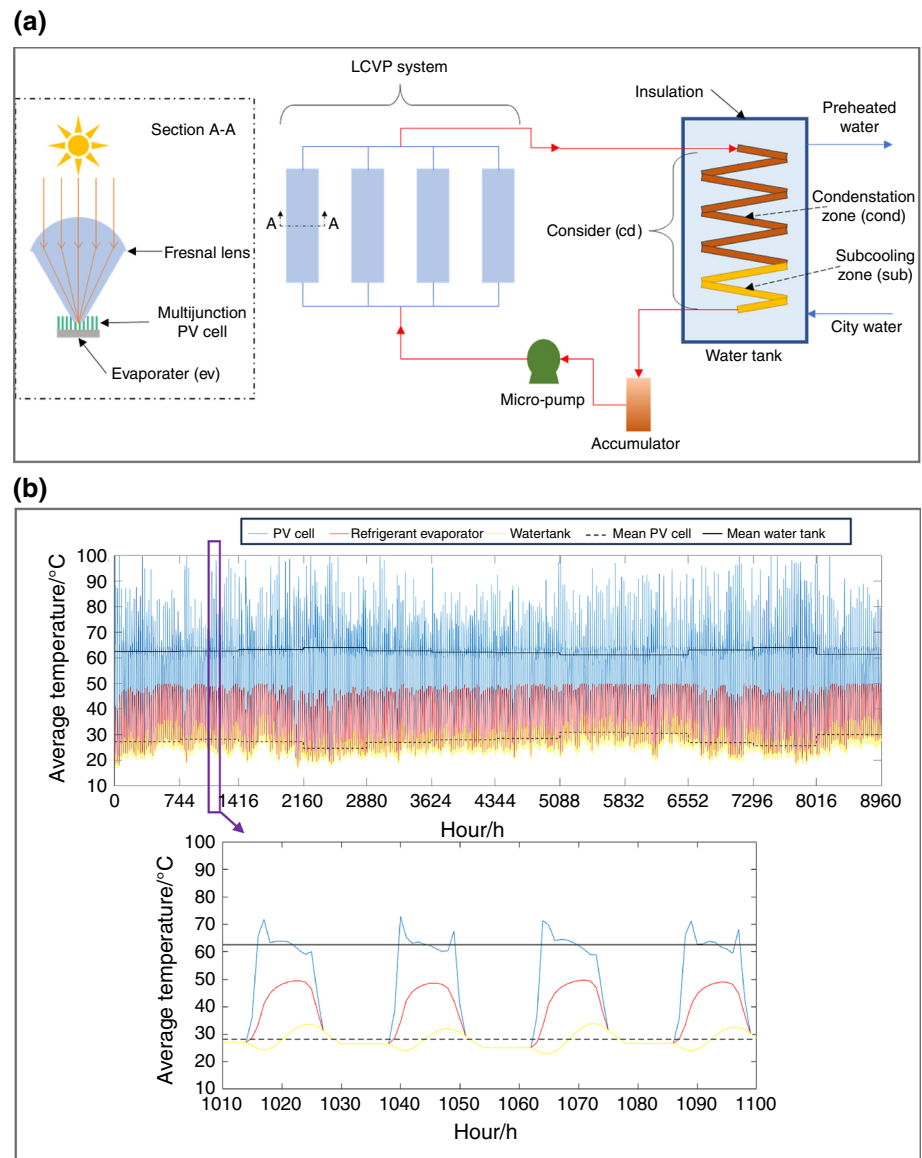


**Fig. 21** **a** Schematic diagram of the low concentrating photovoltaic experimental setup using a two-phase mechanical pump circuit cooling system; **b** Temperature profile for an entire year [31]



study used water as the cooling medium and demonstrated that the 10 PPI functional gradient aluminum foam heat sink, with porosity gradients of 0.794 and 0.682, exhibited minor pressure drop and achieved the highest thermal performance. When the water mass flow rate was  $20 \text{ g}^{-1}$ , the temperature difference of the solar cell, which had a total heat generation of 900 W, was measured to be  $3.9 \text{ }^{\circ}\text{C}$ .

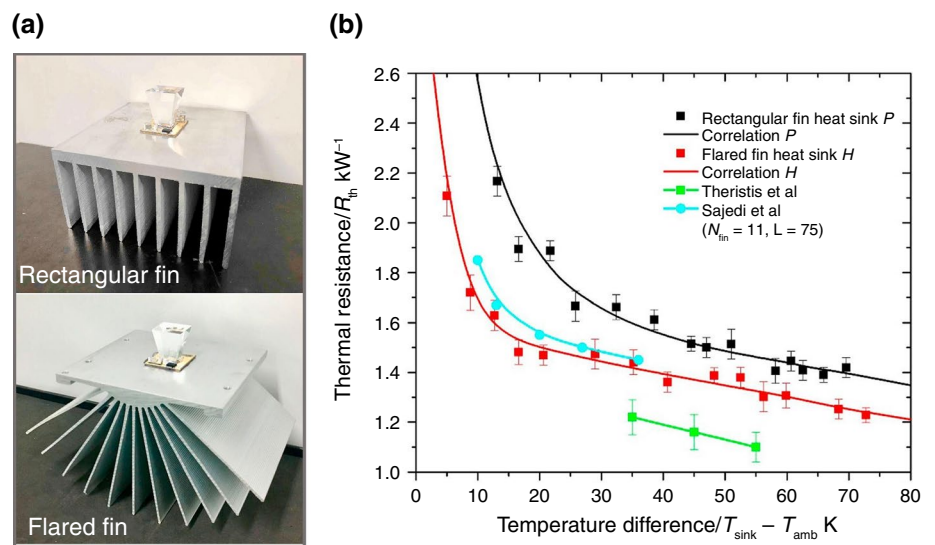
Pabon et al. [31] designed a new cooling method for the LCVP system, the two-phase mechanical pump loop (TMPL), as shown in Fig. 21a. The study results show that using the TMPL system can effectively eliminate the heat generated by the photovoltaic cells, thereby enhancing both temperature stability and efficiency of the cells. As shown in Fig. 21b, the LCPV-TMPL system utilizes four photovoltaic cells with a diameter of 10 mm and a length of 5 m in the case study area. It generates an average monthly power

output of 2 kW and reaches a peak monthly power output of 5 kW, corresponding to an average and peak solar radiation intensity of  $400 \text{ W m}^{-2}$  and  $600 \text{ W m}^{-2}$ . The water tank can heat an average of  $2.2 \text{ m}^3$  per day from  $8 \text{ }^{\circ}\text{C}$  to about  $28 \text{ }^{\circ}\text{C}$ . This means the LCPV-TMPL system can save 9000 kWh and 1900 kWh of electricity and thermal energy (water heating) per year. The system can be used in localized areas with low or moderate solar radiation and cold weather.

### Passive cooling system

In contrast to active cooling systems, passive cooling systems can cool and suppress cell heating in solar panels without requiring an external power source [34, 141]. Passive cooling is less expensive than active cooling but also less efficient [146, 147]. Therefore, passive cooling systems

**Fig. 22** **a** Diagrams of rectangular fin (control group) and flared fin heat sink (experimental group) geometries; **b** The overall thermal resistance differences between the flared fin and the rectangular fin heat sink [148]



are more suitable for LCPV systems. The past 5 years of research on passive cooling technologies have primarily focused on air, PCM, and heat pipe cooling. This section will systematically and comprehensively review the research progress and current status of standard passive cooling technologies in these areas over the last 5 years.

**Air cooling**

Passive air cooling is commonly referred to as fin cooling. Luo et al. [148] proposed an improved expanded fin heat sink, as shown in Fig. 22a. The research results are shown in Fig. 22, indicating a 10% reduction in the total thermal resistance of the flared fin radiator compared to that of the rectangular plate fin radiator. Alzahrani et al. [149] studied the maximum cell temperature of the micro-fin heat sink

with three different substrate materials. The results demonstrate a linear relationship between the cell temperature and the coefficient of thermal resistance, while the ambient temperature remains unaffected by the substrate material. Moreover, when compared to a flat heat sink with directly bonded copper (DBC), an insulated metal substrate (IMS), and Si wafer substrates, the integrated micro-fin heat sink exhibits significantly higher heat dissipation rates of 25.32%, 23.13%, and 22.24%, respectively. This improvement can be attributed to the lower thermal resistance offered by IMS substrates in comparison to DBC and Si wafer substrates, resulting in superior thermal performance that effectively maintains cell temperatures below 80 °C, while accommodating a wider range of high concentrator ratios. Song et al. [150] proposed a heat pump (LCPV/fin-SAHP) system that consists of fins and LCPV, as shown in Fig. 23a. The study

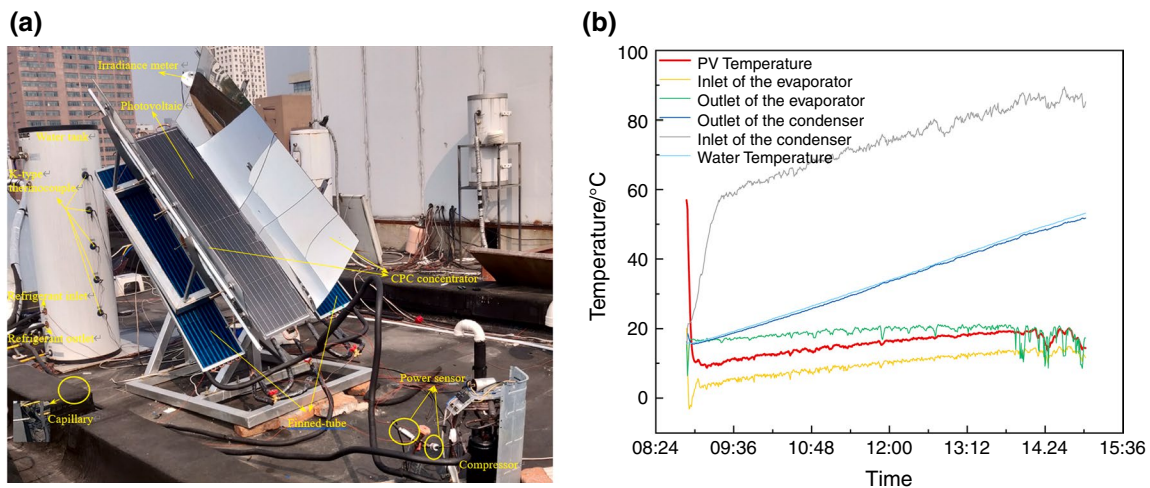


**Fig. 23** **a** Diagram of the experimental setup of the heat pump system; **b** Temperature at different locations [150]

results demonstrated that this method exhibited excellent cooling for CPV, reducing the temperature by approximately 50 °C and increasing the electrical efficiency by 4.6%, as shown in Fig. 23b.

### PCM cooling

Phase change materials (PCMs) are widely recognized as key cooling devices in passive cooling systems, encompassing organic, inorganic, and eutectic compositions [127]. PCMs possess remarkable flexibility and adjustability, enabling efficient thermal energy storage during solar availability and subsequent release when solar energy is scarce. This capability optimizes waste heat utilization while effectively reducing battery temperatures to enhance overall system efficiency [151, 152]. Nevertheless, the implementation of PCM cooling systems remains challenging due to their high cost. Aslfattahi et al. [153] first proposed using novel graphene–silver (Gr–Ag) hybrid nanomaterials combined with paraffin as PCM for CPV/T systems. The results showed that the hybrid graphene–silver nanoparticles exhibited the highest thermal efficiency of 39.62%, which was 4.16% higher than pure PCM. Rejeb et al. [154] investigated the effect of using PCM as a cooling medium on the performance of CPV-TE systems in terms of temperature variation, power generation, and energy efficiency. Under the climatic conditions of Dubai and Naples, the maximum power in the CPV module in the CPVT-TE is 170 W m<sup>-2</sup> and 66 W m<sup>-2</sup> in summer, and 80 W m<sup>-2</sup> and 64 W m<sup>-2</sup> in winter, respectively. Additionally, the TE module generates a maximum power of 1.317 W and 0.127 W during summer and winter, respectively. Yusuf et al. [155] studied and discussed the effect of using different PCMs in CPV, CPV-PCM, CPV-TE, CPV-PCM-TE, and CPV-TE-PCM and PCM containers with different internal configurations on the energy output of the system. The results show that the energy conversion efficiency of CPV-PCM, CPV-TE, CPV-PCM-TE, and CPV-TE-TEM systems is 34.8%, 97.3%, 106.5%, and 114% higher than that of the stand-alone CPV system, respectively. Furthermore, owing to the significant temperature gradient

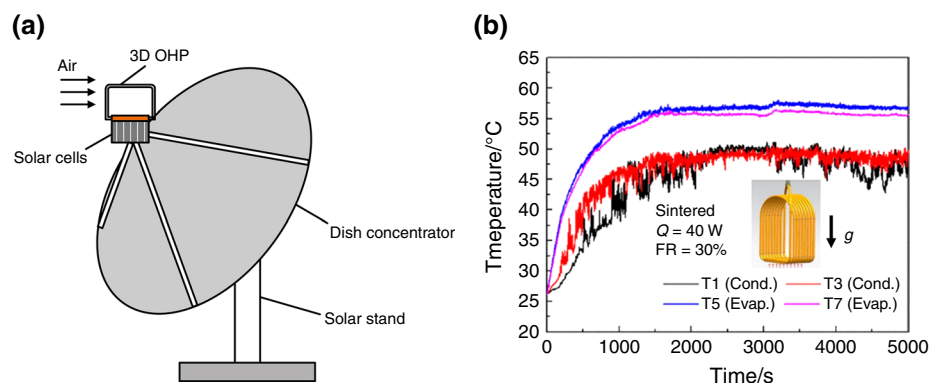
generated within the structure, the CPV-TE-PCM configuration exhibits superior characteristics compared to other forms. Sharma et al. [156] investigated the effect of PCM as a passive cooling technique on the performance of window-integrated concentrated photovoltaic (WICPV) systems. The study results demonstrated that PCM is advantageous for regulating the thermal conditions of WICPV.

### Heat pipe cooling

Heat pipe cooling exhibits exceptional heat transfer capability, cost-effectiveness, and reliability, rendering it a highly efficient cooling solution for CPV systems in recent years [157]. Shittu et al. [158] conducted a study on a hybrid concentrated photovoltaic–thermoelectric design with/without a flat plate heat pipe. The results of the study demonstrated that when concentrator ratio is 6, the efficiency of the photovoltaic–thermoelectric-Heat pipe system was 1.47% and 61.01% higher than that of the photovoltaic–thermoelectric and photovoltaic systems, respectively. Wang et al. [159] proposed an innovative atmospheric plate thermo-siphon (APT) cooling system for efficient heat dissipation in single-concentrating or low-concentrating solar cells. The research findings demonstrate the effectiveness of the APT cooling system in reducing photovoltaic cell temperatures, with a shorter start-up time observed as the heat flow density increases. Soliman et al. [160] investigated the impact of flat-plate heat pipe cooling on the performance of concentrated solar cells, revealing that an increase in the size of the heat pipe condenser and a decrease in the length of the adiabatic zone resulted in higher cell efficiency and output power.

The oscillating heat pipe (OHP) is renowned for its coreless design, which effectively dissipates a substantial amount of heat from high-density solar cells [161–163]. However, there is limited literature on the utilization of OHP as a cooling system in CPV cooling applications. To address this gap, Wang et al. [118] devised and fabricated a three-dimensional OHP featuring a flat plate evaporator, as depicted in Fig. 24a. Subsequently, they conducted

**Fig. 24** **a** Schematic diagram of 3D oscillating heat pipe cooling; **b** Temperature history of evaporator and condenser of 3D oscillating heat pipe with and without sintered copper particles at the vertical orientation ( $Q = 40$  W): sintered, filling ratio of 30% [118]



experimental investigations to evaluate its cooling performance on concentrated photovoltaic cells. The starting performance, effective thermal resistance, and the effect of tilt angle on the thermal performance of oscillating heat with/without sintered copper particles in the evaporator section were compared and evaluated. The results demonstrate that the presence of a porous structure formed by sintered copper particles on the evaporator significantly enhances vapor bubble generation and growth rate, facilitates rapid thin film evaporation formation, and improves latent heat transfer capability. Consequently, it can be concluded that 3D oscillating heat pipes exhibit excellent heat transfer performance and are well-suited for cooling concentrated photovoltaic systems, as shown in Fig. 24b.

## Hybrid cooling techniques

### Active + passive cooling

The impact of each cooling medium on the CPV system is positive; however, their effects vary to some extent. Combining active and passive cooling techniques can effectively mitigate the temperature influence on photovoltaic panels [164, 165]. Therefore, Ji et al. [166] conducted a comparative study of CPV systems employing three prevalent active cooling techniques: air-cooled, water-cooled, and heat pipe cooling. The findings of the investigation demonstrate that the CPV cell integrated with heat pipe cooling exhibits superior output power. Considering pump consumption, however, the water-cooled CPV cell demonstrates optimal net electrical efficiency and electrical energy efficiency. Kouravand et al. [167] investigated five cooling methods for CPV systems, including water circulation CPV-T (CPV-T/W), nanofluid circulation CPV-T (CPV-T/NF), nanofluid and PCM mixed circulation CPV-T (CPV-T/NF/PCM), nanofluid and finned PCM combined circulation CPV-T (CPV-T/NF/FPCM) and water circulation and finned PCM mixed circulation CPV-T (CPV-T/W/FPCM). This indicates that the best cooling performance was achieved by the CPVT-NF-FPCM method under experimental conditions, which can narrow down the technology gap of using PCM, metal fins, and nanofluids in CPVT systems. Soliman et al. [168] investigated the effect of the heatsink (H.S.) size, microchannel (mic) structure, and the use of nanoparticles on the cooling CPV performance of the heatsink-microchannel system. The results demonstrate that the incorporation of SiC nanoparticles in conjunction with cooling water within the mic enhances photovoltaic efficiency and mitigates both the maximum photovoltaic temperature and temperature variation on the photovoltaic surface. During experimentation, a spreader was interposed between the photovoltaic and the mic. Increasing the area ratio (A.R.) of this spreader to the photovoltaic leads to

improvements in photovoltaic efficiency, output power, and temperature uniformity. Under similar flow conditions, compared to water without SiC NPs, incorporating SiC nanoparticles resulted in a net capacity increase of 9.2% at A.R. = 1 and 0.3% at A.R. = 7 when  $Re = 5$ ; as well as an increase of 2.6% at A.R. = 1 and 1.5% at A.R. = 7 when  $Re = 85$ .

Nasef et al. [169] developed an integrated passive and active cooling system for the thermal regulation of CPV solar systems, which combines a PCM thermal storage cell with a closed-loop water/nanofluid cooling system. The study results demonstrate that compared to conventional direct PCM- photovoltaic and water-cooled stand-alone systems, the average CPV temperature can be reduced by 60%. Rahmanian et al. [170] proposed to combine a novel PCM heat sink with a building-integrated concentrated photovoltaic (BICPV) system. The study findings demonstrate the effective enhancement of both electrical and thermal efficiency in the system, attributed to the increased thermal conductivity. Torbatinezhad et al. [171] introduced a wave-shaped small channel radiator mixed with a jet impingement cooling system. The experimental results demonstrate that the microchannel wavelength can be reduced from 12.5 to 5 mm at a mass flow rate ( $\dot{m}$ ) of  $0.08 \text{ kg s}^{-1}$ , leading to an average temperature reduction of 4.46% and an enhanced performance improvement of 28.77%. Furthermore, increasing the coolant rate from  $\dot{m} = 0.05 \text{ kg s}^{-1}$  to  $\dot{m} = 0.15 \text{ kg s}^{-1}$  resulted in a temperature decrease of approximately  $12 \text{ }^\circ\text{C}$  at a  $30^\circ$  impact angle, accompanied by an impressive electrical efficiency reaching up to 29.65%. Torbatinezhad et al. [172] proposed a jet impingement/small channel heat dissipation model to enhance the surface temperature reduction of triple-junction solar cells in a flat-plate concentrating solar system. The study findings demonstrate that the utilization of a pin-fin reinforced heat sink improves the heat transfer characteristics compared to a simple heat sink. Increasing the angle of the heat sink from  $0^\circ$  to  $40^\circ$  resulted in a decrease in temperature from 321.9 to 321.2 K, thereby enhancing electrical efficiency up to 28.95%.

### Thermoelectric system

The utilization of a semiconductor device thermoelectric generator (TEG) enables the generation of electrical energy by harnessing the temperature difference between its surfaces [173]. Consequently, integrating TEG and CPV systems within a CPV/not only facilitates passive cooling of solar cells but also yields additional thermoelectric power [146]. Sabry et al. [174] investigated the system performance of three TEG modules with varying sizes and node quantities. The findings demonstrate that the proposed hybrid concentrating photovoltaic/thermoelectric generator

(CPV/TEG) system outperforms the CPV-only system in terms of net power generation. Specifically, the power output of the hybrid CPV/TEG system exhibited an increase of 7.4%, 5.8%, and 3%, respectively, compared to a scenario where only a CPV cell was installed on top of the radiator. Lekbir et al. [175] investigated a hybrid cooling system based on nanofluid concentrating photovoltaic/thermoelectric generator (NCPV/T-TEG). The findings demonstrate an enhancement in the electrical performance of the NCPV/T-TEG structure, with improvements of 89% compared to standard photovoltaic modules, approximately 13.9% compared to CPV/TEG, and around 8.4% compared to water cooling. Rodrigo et al. [176] initially conducted an analysis on the potential of CPV/TEG systems for passive cooling technologies and subsequently developed an electrical/thermal/economic model for concentrating photovoltaic–thermoelectric modules. The study findings demonstrate that the proposed model exhibits a significant enhancement in efficiency and cost reduction compared to conventional CPV modules with 800× light gathering factor and 36.4% efficiency. Hajji et al. [177] proposed an efficient cooling system using indirectly coupled CPV mixed with concentrated thermoelectric (CTE) modules. In their study, the performance of the CPV/CTE system was investigated using both nanofluid and water as cooling media separately. The results demonstrated that incorporating copper-based nanofluid as a coolant could significantly enhance the efficiency of this hybrid system compared to conventional water cooling methods. Specifically, the hybrid CPV system achieved a remarkable 10% increase in overall efficiency when compared to typical CPV systems. Lekbir et al. [178] proposed a new configuration of a NCPV/T-TEG hybrid system with cooling channels. The obtained results demonstrate that the electrical energy output of the NCPV/T-TEG structure surpasses that of NCPV/T, CPV, and CPV/TEG-HS systems by 10%, 47.7%, and 49.5%, respectively, at both the optimum concentrator ratio value and maximum operating temperature.

The combination of a CPV system and a photovoltaic/thermal system offers the advantages of both technologies [26, 179]. In an open-air environment, Kong et al. [180] investigated the effect of different heat sinks (*s*-type and *h*-type) on the photothermal, photovoltaic, and cogeneration performance of a composite parabolic concentrated photovoltaic/thermal phase change system. The results show that the *h*-type heat sink system with integrated PCM performs better temperature regulation. In contrast, the CPV/T phase change system with an *s*-type heat sink shows excellent potential in terms of cogeneration performance. Rejeb et al. [181] investigated the effect of water-containing and 0.5% graphene/water nanofluid charged as a coolant on the performance of CPV/T-TE systems, respectively. The results showed that the total electrical power and

exergy increased. In contrast, the thermal energy decreased significantly for CPV/T-TE and CPV/T-TE with 0.5% graphene/water nanofluid addition compared to the CPV/T system. However, the utilization of full-spectrum solar radiation in a CPV/T system may result in an elevation of system temperature. Therefore, timely removal of waste heat is necessary and can be achieved through a coupled cooling/thermal system or by splitting the full spectrum solar energy into two parts using a beam splitter. The high-frequency part is then directed to the concentrating photovoltaic module, while the remaining portion is utilized by the near-field thermal photovoltaic module. A spectroscopic beam splitter utilizes the spectral splitting capability of a substance to effectively lower the temperature of a photovoltaic cell [182, 183]. Selective absorption coating represents one form of SBS that has been employed. However, limitations such as high cost and susceptibility to degradation hinder its widespread application. To address this issue, Alzahrani et al. [184] proposed employing graphene as an illumination-cooling technique for solar cells. The findings demonstrated that incorporating graphene as a neutral density filter component reduced the geometric concentrator ratio and enhanced the efficiency of solar cells.

Fluid-selective absorption filters represent an alternative approach to utilizing selective absorption coatings. Distinguished from the latter, fluid-selective absorption spectrometers can serve as both a cooling medium and a spectrometer in CPV systems [179, 184]. Han et al. [185] proposed a CPV/T system that consists of an/CoSO<sub>4</sub>-propylene glycol nanofluid spectroscopic beam splitter and utilizes heat pipe cooling technique. The study also discussed the impact of heat pipe cooling on the performance of the nanofluid spectroscopic beam-splitting system. The results show that, on average, there is a 10.4% difference in total efficiency between the system with heat pipe cooling and without it when varying the concentrator ratio from 1 to 8 Suns. At a typical daily solar irradiance with a concentrator ratio of 5 Suns, the instantaneous total efficiency reaches its maximum at 73.20% at 17:00, with electricity contributing to 7.55%, and the average total efficiency for the entire day is 53.66%. Meraje et al. [186] investigated the use of ZnO nanofluid as a beam splitter for CPV/T systems to achieve full spectrum utilization. The results showed that the combined efficiency of CPV/T was 50.35%, 65.2%, 72.70%, 74.7%, and 85% for ZnO nanofluids with volume concentrations of 0.00036%, 0.00089%, 0.0017%, 0.0036%, and 0.0089%, respectively. Lin et al. [187] proposed a two-stage concentrated split photovoltaic/thermal system based on nanofluid, which achieves a thinner split layer of optical nanofluid and effective thermal management. The study results show that the two-stage robust split photovoltaic/thermal system without cooling channels improves thermal efficiency by 1.4% and 2.9%, respectively, compared to the conventional split

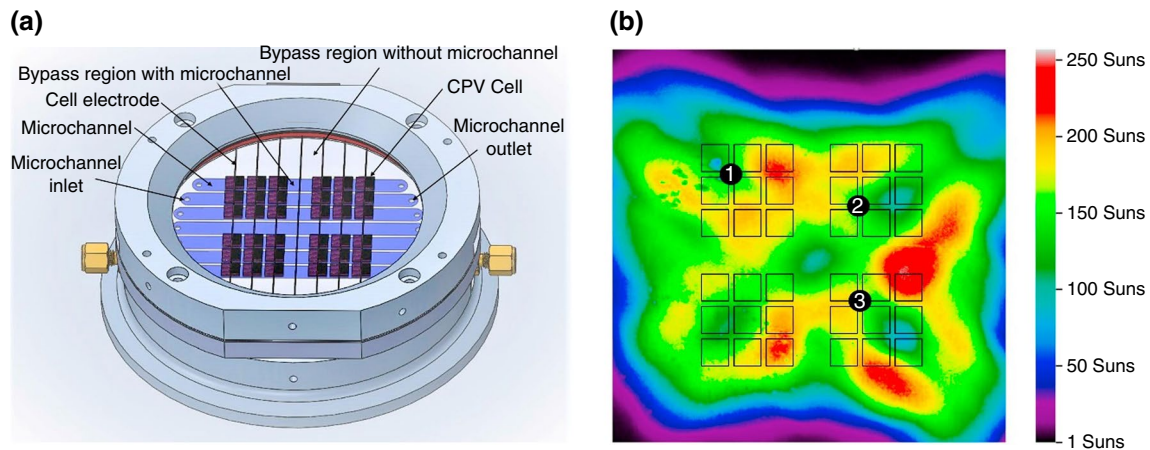


**Fig. 25** **a** Schematic diagram of the structure of a transmissive active cooling system in a concentrating photovoltaic/thermal system; **b** Map showing distribution of solar energy flux on the concentrating photovoltaic module [124]

photovoltaic/thermal system. Not only does it achieve high-temperature protection of nanofluid, but also the flexible hybrid system has an output power that is 14.3% and 10% higher than that of the conventional photovoltaic/thermal system without cooling concentrated split photovoltaic/thermal system, respectively. Anand et al. [188] proposed a hybrid system that combines a CPV/T system with a desalination and cooling unit to fully utilize solar energy. The CPV/T system provides hot water for HDH desalination and electrical power for the vapor compression refrigeration system. The study results showed that coupling a CPVT system with a desalination and cooling unit increased the energy utilization factor (EUF) of the unit. The highest increase in the EUF of the electric field was 49% at a hot water temperature of 47.5 °C. Islam et al. [124] proposed a transmissive active cooling system for hybrid spectroscopic CPV/T systems, as shown in Fig. 25a. The study results showed that the cooling channel maintained the temperature of the CPV cell below 69 °C during a concentrated test with 175 Suns. The experimentally validated model predicted, as shown in Fig. 25b, that the cell temperature would remain below the maximum temperature of 110 °C even at high concentrations of up to 665 Suns.

## Conclusions

Compared to photovoltaic systems, CPV systems offer significant advantages in cost reduction and more efficient solar energy collection. This paper aims to enhance the overall efficiency of CPV systems by addressing the temperature effect. We review and discuss the key components influencing the temperature effect of CPV systems, along with corresponding solution measures and research progress in this field. The main steps proposed

for mitigating the temperature effect of CPV systems include improvements in solar concentrators, solar tracking systems, and cooling mechanisms. The review presents a comprehensive exposition of these three recommendations. The subsequent deductions can be derived from this article:

1. The solar concentrator serves as the fundamental component of the CPV system and plays a crucial role in its temperature effect, leading to an increase in surface temperature of the solar cell with intensified concentrated light. Additionally, solar concentrators concentrate dispersed sunlight onto the solar cell, resulting in nonuniform radiation across its surface. Consequently, optimizing and designing the concentrator becomes imperative for mitigating the temperature effect of CPV systems. This review paper comprehensively examines various types of solar concentrators including Fresnel, Dish, composite parabolic troughs, and trough concentrators. design process, researchers primarily focus on investigating how concentration ratio impacts both optical and electrical performance of CPV systems while also developing accurate predictive models and implementing measures to minimize their temperature effect.
2. Conventional CPV systems feature stationary panels that lack sun-tracking capabilities, resulting in limited daily solar energy intake and suboptimal utilization of solar single-axis and dual-axis solar trackers has significantly enhanced the efficiency of CPV systems. Further research on solar trackers should focus on investigating the impact of wind speed, module angle, and other factors on tracker performance.
3. The cooling system is considered one of the most effective thermal management methods for enhancing the temperature performance of CPV systems. These

systems can be categorized into active, passive, and hybrid cooling systems based on their reliance on an external power supply. Active cooling systems are typically employed in HCPV systems, while LCPV systems commonly utilize passive cooling techniques. Researchers have extensively explored active cooling approaches such as liquid cooling, microchannel heat dissipation, and nano-fluid cooling. Noteworthy advancements in active cooling methods include buried water heat exchangers, silicone oil applications, metal foam heat sinks, and two-phase mechanical pump circuits.

4. Nanofluid cooling is an emerging technology in active cooling systems, which can serve as a coolant in CPV systems and a spectrometer in CPV/T systems. However, the spectral response and absorption properties of nanofluids are influenced by factors such as nanoparticle size, concentration, and type. Therefore, it is crucial to fully consider these factors when studying nanofluids. Nevertheless, long-term stability remains a challenge for nanofluids currently. Research on passive cooling technologies has primarily focused on three areas: air cooling, phase change materials (PCM) cooling, and heat pipe cooling. PCM cooling shows promising potential but still faces the limitation of high cost.
5. The hybridization of active and passive cooling systems can effectively overcome the limitations imposed by a single cooling medium, thereby combining the advantages offered by two or more media. This approach leads to a significant reduction in the temperature impact on CPV systems. Moreover, the integration of thermoelectric cogeneration system not only maximizes the utilization of waste heat generated by CPV systems but also substantially lowers the surface temperature of PV panels. Consequently, it enhances overall efficiency and facilitates comprehensive exploitation of solar energy resources.

In conclusion, the elimination of temperature effects in CPV systems remains a technological challenge yet to be overcome. Based on the literature review, it is evident that the most effective approach to mitigate these effects involves optimizing and designing the solar concentrator, tracker, and cooling system separately. However, this coupling strategy necessitates higher construction costs and increased maintenance complexity. Therefore, future research should prioritize mitigating the adverse effects of elevated temperatures on CPV systems. This can be achieved through the implementation of cogeneration or the utilization of thermoelectric materials for efficient heat and waste heat harvesting, thereby ensuring optimal energy utilization. Additionally, it is crucial to assess the economic feasibility

and practical benefits of these approaches in real-life engineering applications.

**Acknowledgements** This work was funded by the National Natural Science Foundation of China (52106099), the Taishan Scholars Program.

**Data availability** Data will be made available on request.

## Declarations

**Conflict of interest** The authors declare that they have no known competing financial interests or personal relationships that could have appeared to influence the work reported in this paper.

## References

1. Tzeremes P, Dogan E, Alavijeh NK. Analyzing the nexus between energy transition, environment and ICT: a step towards COP26 targets. *J Environ Manag.* 2023;326:116598.
2. Stavi I. Rio (1992) to Glasgow (2021): three decades of inadequate mitigation of climate change and its slow onset effects. *Front Environ Sci.* 2022;10:999788.
3. Yan Q, Wang Y, Li Z, Baležentis T, Streimikiene D. Coordinated development of thermal power generation in Beijing–Tianjin–Hebei region: evidence from decomposition and scenario analysis for carbon dioxide emission. *J Clean Prod.* 2019;232:1402–17.
4. Yu J, Tang YM, Chau KY, Nazar R, Ali S, Iqbal W. Role of solar-based renewable energy in mitigating CO<sub>2</sub> emissions: Evidence from quantile-on-quantile estimation. *Renew Energy.* 2022;182:216–26.
5. PraveenKumar S, Agyekum EB, Kumar A, Velkin VI. Performance evaluation with low-cost aluminum reflectors and phase change material integrated to solar PV modules using natural air convection: an experimental investigation. *Energy.* 2023;266:126415.
6. Zhang X, Zhang H, Zhao C, Yuan J. Carbon emission intensity of electricity generation in Belt and Road Initiative countries: a benchmarking analysis. *Environ Sci Pollut Res.* 2019;26:15057–68.
7. Hayat MB, Ali D, Monyake KC, Alagha L, Ahmed N. Solar energy—a look into power generation, challenges, and a solar-powered future. *Int J Energy Res.* 2018;43:1–19.
8. Coffel ED, Mankin JS. Thermal power generation is disadvantaged in a warming world. *Environ Res Lett.* 2021;16:024043.
9. Wang S, Zhu X, Song D, Wen Z, Chen B, Feng K. Drivers of CO<sub>2</sub> emissions from power generation in China based on modified structural decomposition analysis. *J Clean Prod.* 2019;220:1143–55.
10. Asselt H, Green F. COP26 and the dynamics of anti-fossil fuel norms. *WIREs Clim Change.* 2022;14:e816.
11. Zou Y, Li XK, Yang L, Zhang B, Wu XH. Efficient direct absorption solar collector based on hollow TiN nanoparticles. *Int J Therm Sci.* 2023;185:108009.
12. Emodi NV, Chaiechi T, Alam Beg ABMR. The impact of climate variability and change on the energy system: a systematic scoping review. *Sci Total Environ.* 2019;676:545–63.
13. Abudurehman M, Jiang Q, Dong X, Dong C. CO<sub>2</sub> emissions in China: Does the energy rebound matter? *Energies.* 2022;15:4279.
14. Victoria M, Haeger N, Peters IM, Sinton R, Jäger-Waldau A, Cañizo C, Breyer C, Stocks M, Blakers A, Kaizuka I, Komoto



- K, Smets A. Solar photovoltaics is ready to power a sustainable future. *Joule*. 2021;5:1–16.
15. Praveenkumar S, Agyekum EB, Kumar A, Velkin VI. Thermo-economic analysis of solar photovoltaic/thermal system incorporated with u-shaped grid copper pipe, thermal electric generators and nanofluids: an experimental investigation. *J Energy Storage*. 2023;60:106611.
  16. Becquerel M, Hebd CR. *Séances l'Acad. Science*. 1839;9:561.
  17. Lee SW, Bae S, Kim D, Lee HS. Historical analysis of high-efficiency, large-area solar cells: toward upscaling of perovskite solar cells. *Adv Mater*. 2020;32:2002202.
  18. Sun C, Zou Y, Qin C, Zhang B, Wu X. Temperature effect of photovoltaic cells: a review. *Adv Compos Hybrid Mater*. 2022;5:2675–99.
  19. Dedović MM, Avdaković S, Mujezinović A, Dautbašić N. Integration of PV into the Sarajevo Canton energy system-air quality and heating challenges. *Energies*. 2021;14:123.
  20. Hasan A, Sarwar J, Shah AH. Concentrated photovoltaic: a review of thermal aspects, challenges and opportunities. *Renew Sustain Energy Rev*. 2018;94:835–52.
  21. Borba B, Henrique SMCLF, Malagueta DC. A novel stochastic optimization model to design concentrated photovoltaic/thermal systems: a case to meet hotel energy demands compared to conventional photovoltaic system. *Energy Convers Manag*. 2020;224:113383.
  22. Ejaz A, Babar H, Ali H, Jamil F, Janjua M, Fattah IMR, Said Z, Li CH, Janjua MM, Rizwanul Fattah IM, Said Z, Li C. Concentrated photovoltaics as light harvesters: outlook, recent progress, and challenges. *Sustain Energy Technol Assess*. 2021;46:101199.
  23. Garcia AB, Voarino P, Raccurt O. Environments, needs and opportunities for future space photovoltaic power generation: a review. *Appl Energy*. 2021;290:116757.
  24. Alves M, Pérez-Rodríguez A, Dale PJ, Domínguez C, Sadewasser S. Thin-film micro-concentrator solar cells. *J Phys Energy*. 2020;2:012001.
  25. Papis-Frączek K, Sornek K. A review on heat extraction devices for CPVT systems with active liquid cooling. *Energies*. 2022;15:6123.
  26. Alzahrani M, Shanks K, Mallick TK. Advances and limitations of increasing solar irradiance for concentrating photovoltaics thermal system. *Renew Sustain Energy Rev*. 2021;138:110517.
  27. Sato D, Tanino K, Yamada N. Thermal characterization of a silicone-on-glass micro aspheric lens array for a concentrator photovoltaic module. *Sol Energy Mater Sol Cells*. 2020;208:110396.
  28. Han X, Lv Y. Design and dynamic performance of a concentrated photovoltaic system with vapor chambers cooling. *Appl Therm Eng*. 2022;201:117824.
  29. Fernández EF, Almonacid F, Rodrigo PM, Pérez-Higueras PJ. Chapter II-4-A—CPV systems. In: Kalogirou SA, editor. *McEvoy's handbook of photovoltaics*. 3rd ed. Cambridge: Academic Press; 2018. p. 931–85.
  30. Sadhukhan P, Roy A, Sengupta P, Das S, Mallick TK, Nazeeruddin MK, Sundaram S. The emergence of concentrator photovoltaics for perovskite solar cells. *Appl Phys Rev*. 2021;8:041324.
  31. Li G, Xuan Q, Pei G, Su Y, Ji J. Effect of non-uniform illumination and temperature distribution on concentrating solar cell—a review. *Energy*. 2018;144:1119–36.
  32. Pabon JGG, Khosravi A, Malekan M, Sandoval OR. Modeling and energy analysis of a linear concentrating photovoltaic system cooled by two-phase mechanical pumped loop system. *Renew Energy*. 2020;157:273–89.
  33. Alamoudi A, Saaduddin SM, Munir AB, Muhammad-Sukki F, Abu-Bakar SH, Yasin SHM, Karim R, Bani NA, Mas'ud AA, Ardila-Rey JA, Prabhu R, Sellami N. Using static concentrator technology to achieve global energy goal. *Sustainability*. 2019;11:3056.
  34. Gharzi M, Arabhosseini A, Gholami Z, Rahmati MH. Progressive cooling technologies of photovoltaic and concentrated photovoltaic modules: a review of fundamentals, thermal aspects, nanotechnology utilization and enhancing performance. *Sol Energy*. 2020;211:117–46.
  35. Tina GM, Ventura C, Ferlito S, Vito SD. A state-of-art-review on machine-learning based methods for PV. *Appl Sci*. 2021;11:7550.
  36. Ziemińska-Stolarska A, Pietrzak M, Zbiciński I. Application of LCA to determine environmental impact of concentrated photovoltaic solar panels—state-of-the-Art. *Energies*. 2021;14:3143.
  37. Ibrahim KA, Luk P, Luo Z. Cooling of concentrated photovoltaic cells—a review and the perspective of pulsating flow cooling. *Energies*. 2023;16:2842.
  38. Praveenkumar S, Agyekum EB, Kumar A, Ampah JD, Afrane S, Amjad F, Velkin VI. Techno-economics and the identification of environmental barriers to the development of concentrated solar thermal power plants in India. *Appl Sci*. 2022;12:10400.
  39. Himer SE, Ayane SE, El-Yahyaoui S, Salvestrini JP, Ali A. Photovoltaic concentration: research and development. *Energies*. 2020;5721:13.
  40. Felsberger R, Buchroithner A, Gerl B, Wegleiter H. Conversion and testing of a solar thermal parabolic trough collector for CPV-T application. *Energies*. 2020;13:6142.
  41. Gonzalo AP, Marugán AP, García Márquez FP. A review of the application performances of concentrated solar power systems. *Appl Energy*. 2019;255:113893.
  42. Masood F, Nor NBM, Elamvazuthi I, Saidur R, Alam MA, Akhter J, Yusuf M, Ali SM, Sattar M, Baba M. The compound parabolic concentrators for solar photovoltaic applications: opportunities and challenges. *Energy Rep*. 2022;8:13558–84.
  43. Awasthi K, Reddy DS, Khan MK. Design of Fresnel lens with spherical facets for concentrated solar power applications. *Int J Energy Res*. 2019;44:1–13.
  44. Desnijder K, Hanselaer P, Meuret Y. Freeform Fresnel lenses with a low number of discontinuities for tailored illumination applications. *Opt Express*. 2020;28:24489.
  45. Li X, Lan T, Wang Y, Wang LH. Design and study of Fresnel lens for an antenna in indoor visible light communication system. *Acta Phys Sin Ch Ed*. 2015;64:024201.
  46. Wang D, Lin P, Chen Z, Fei C, Qiu Z, Chen Q, Sun X, Wu Y, Sun L. Evolvable acoustic field generated by a transducer with 3D-Printed Fresnel lens. *Micromachines*. 2021;12:1315.
  47. Wang G, Wang F, Shen F, Jiang T, Chen Z, Hu P. Experimental and optical performances of a solar CPV device using a linear Fresnel reflector concentrator. *Renew Energy*. 2020;146:2351–61.
  48. Vu DT, Vu NH, Shin S, Pham TT. Cylindrical Fresnel lens: an innovative path toward a tracking-less concentrating photovoltaics system. *Sol Energy*. 2022;234:251–61.
  49. Ahmadpour A, Dejamkhooy A, Shayeghi H. Optimization and modelling of linear Fresnel reflector solar concentrator using various methods based on Monte Carlo Ray-Trace. *Sol Energy*. 2022;245:67–79.
  50. Wang G, Shen F, Wang F, Chen Z. Design and experimental study of a solar CPV system using CLFR concentrator. *Sustain Energy Technol Assess*. 2020;40:100751.
  51. Alamri YA, Mahmoud S, Al-Dadah R, Sharma S, Roy JN, Ding Y. Optical performance of single point-focus fresnel lens concentrator system for multiple multi-junction solar cells—a numerical study. *Energies*. 2021;14:4301.
  52. Wu SY, Duan SZ, Xiao L. Thermal, electrical and structural characteristics under different concentrator positions for

- Fresnel concentrating photovoltaic system. *Case Stud Therm Eng.* 2023;41:102597.
53. Kumar KH, Daabo AM, Karmakar MK, Hirani H. Solar parabolic dish collector for concentrated solar thermal systems: a review and recommendations. *Environ Sci Pollut Res.* 2022;29:32335–67.
  54. Zheng T, Zheng F, Rui X, Ji X, Niu K. A novel ultralight dish system based on a three-extensible-rod solar tracker. *Sol Energy.* 2019;193:335–59.
  55. Lokeswaran S, Mallick TK, Reddy KS. Design and analysis of dense array CPV receiver for square parabolic dish system with CPC array as secondary concentrator. *Sol Energy.* 2020;199:782–95.
  56. Pan X, Ju X, Xu C, Du X, Yang Y. A novel rotational symmetry (RS) connection approach for dense-array concentrator photovoltaic (DA-CPV) modules. *Energy Convers Manag.* 2019;181:359–71.
  57. Thirunavukkarasu V, Cheralathan M. An experimental study on energy and exergy performance of a spiral tube receiver for solar parabolic dish concentrator. *Energy.* 2020;192:116635.
  58. Yan J, Liu Y, Peng YD. Study on the optical performance of novel dish solar concentrator formed by rotating array of plane mirrors with the same size. *Renew Energy.* 2022;195:416–30.
  59. Sahu SKAS, Natarajan SK. Design and development of a low-cost solar parabolic dish concentrator system with manual dual-axis tracking. *Int J Energy Res.* 2020;45:1–11.
  60. Liu Y, Peng Y, Yan J. Effect of the azimuth axis tilt error on the tracking performance of a solar dish concentrator system. *Energies.* 2022;15:3261.
  61. Chandan, Baig H, Tahir A, Reddy KS, Mallick TK, Pesala B. Performance improvement of a desiccant based cooling system by mitigation of non-uniform illumination on the coupled low concentrating photovoltaic thermal units. *Energy Convers Manag.* 2022;257:115438.
  62. Lv J, Xu X, Yin P. Design method of a planar solar concentrator for natural illumination. *Sol Energy.* 2019;194:554–62.
  63. Paul DI. Application of compound parabolic concentrators to solar photovoltaic conversion: a comprehensive review. *Int J Energy Res.* 2019;43:1–48.
  64. Chandan Dey S, Kumar PS, Reddy KS, Pesala B. Optical and electrical performance investigation of truncated 3X non-imaging low concentrating photovoltaic–thermal systems. *Energy Convers Manag.* 2020;220:11305.
  65. Zhang G, Wei J, Zhang L, Xi C, Ding R, Wang Z, Khalid M. A comprehensive study on the effects of truncation positions of the compound parabolic concentrator eliminating multiple reflections on the performances of concentrating photovoltaic and thermal system. *Appl Therm Eng.* 2021;183:116162.
  66. Parthiban A, Mallick TK, Reddy KS. Integrated optical-thermal-electrical modeling of compound parabolic concentrator based photovoltaic–thermal system. *Energy Convers Manag.* 2022;251:115009.
  67. Zhang G, Wei J, Wang Z, Xie H, Xi Y, Khalid M. Investigation into effects of non-uniform irradiance and photovoltaic temperature on performances of photovoltaic/thermal systems coupled with truncated compound parabolic concentrators. *Appl Energy.* 2019;250:245–56.
  68. Meng X, Ren FP, Zhang P, Tang Z. Trough-type free-form secondary solar concentrator for CPV/T application. *Energies.* 2022;15:8023.
  69. Otanicar TP, Wingert R, Orosz M, McPheeters C. Concentrating photovoltaic retrofit for existing parabolic trough solar collectors: Design, experiments, and leveled cost of electricity. *Appl Energy.* 2020;265:114751.
  70. Ullah I. Optical modeling of two-stage concentrator photovoltaic system using parabolic trough. *J Photonics Energy.* 2019;9:043102–043102.
  71. Iqbal W, Ullah I, Shin S. Nonimaging high concentrating photovoltaic system using trough. *Energies.* 2023;16:1336.
  72. Qu W, Xing X, Cao Y, Liu T, Hong H, Jin H. A concentrating solar power system integrated photovoltaic and mid-temperature solar thermochemical processes. *Appl Energy.* 2020;262:11442.
  73. Chana W, Wang Z, Yang C, Yuan T, Tian R. Optimization of concentration performance at focal plane considering mirror refraction in parabolic trough concentrator. *Energy Source Part A.* 2022;44:3692–707.
  74. Gong J, Wang J, Hu X, Li Y, Jian H, Wang J, Lund PD, Gao C. Optical, thermal and thermo-mechanical model for a larger-aperture parabolic trough concentrator system consisting of a novel flat secondary reflector and an improved absorber tube. *Sol Energy.* 2022;240:376–87.
  75. Rehman N, Uzair M. Concentrator shape optimization using particle swarm optimization for solar concentrating photovoltaic applications. *Renew Energy.* 2022;184:1043–54.
  76. Alqurashi MM, Ganash EA, Altuwirqi RM. Simulation of a low concentrator photovoltaic system using COMSOL. *Appl Sci.* 2022;12:3450.
  77. Río SB, Osorio-Gómez G. Influence of an anti-reflective coating (ARC) with a pyramidal texture on a building integrated low-concentration photovoltaic (BICPV) system. *Energy Sustain Dev.* 2022;71:222–37.
  78. Alqurashi MM, Altuwirqi RM, Ganash EA. Thermal profile of a low-concentrator photovoltaic: a COMSOL simulation. *Int J Photoenergy.* 2020;2020:1–9.
  79. Alnajideen M, Gao M. A new configuration of V-trough concentrator for achieving improved concentration ratio of >3.0x. *Sol Energy Mater Sol Cells.* 2022;245:111877.
  80. Narasimman K, Kannapan BA, Selvarasan I. Performance analysis of 1-Sun and 2-Sun ridge concentrator PV system with various geometrical conditions. *Int J Energy Res.* 2021;45:1–18.
  81. Ustaoglu A, Ozbey U, Torlakli H. Numerical investigation of concentrating photovoltaic/thermal (CPV/T) system using compound hyperbolic trumpet, V-trough and compound parabolic concentrators. *Renew Energy.* 2020;152:1192–208.
  82. Wei AC, Hsiao SY, Sze JR, Lee JY. V-groove and parabolic array for enlarging the acceptance angle of a side-absorption concentrated photovoltaic system. *Opt Laser Technol.* 2019;112:426–35.
  83. Wang G, Wang F, Chen Z, Hu P, Cao R. Experimental study and optical analyses of a multi-segment plate (MSP) concentrator for solar concentration photovoltaic (CPV) system. *Renew Energy.* 2019;134:284–91.
  84. Xu S, Zhu Q, Hu Y, Zhang T. Design and performance research of a new non-tracking low concentrating with lens for photovoltaic systems. *Renew Energy.* 2022;192:174–87.
  85. Kolamroudi MK, Ilkan M, Egelioglu F, Safaei B. Maximization of the output power of low concentrating photovoltaic systems by the application of reflecting mirrors. *Renew Energy.* 2022;189:822–35.
  86. Ayane SE, Ahaitouf A. Performance analysis of a ball lens as secondary optical element for a micro photovoltaic concentrator. *Energy Rep.* 2022;8:1301–13.
  87. Rafiee M, Chandra S, Ahmed H, McCormack SJ. An overview of various configurations of luminescent solar concentrators for photovoltaic applications. *Opt Mater.* 2019;91:212–27.
  88. Delgado-Sanchez JM, Lillo-Bravo I, Menéndez-Velázquez A. Enhanced luminescent solar concentrator efficiency by Foster resonance energy transfer in a tunable six-dye absorber. *Int J Energy Res.* 2021;45:1–11.

89. Nie Y, He W, Liu X, Hu Z, Yu H, Liu H. Smart luminescent solar concentrator as a BICPV window. *Build Simul.* 2022;15:1789–98.
90. Qu W, Hong H, Jin H. A spectral splitting solar concentrator for cascading solar energy utilization by integrating photovoltaics and solar thermal fuel. *Appl Energy.* 2019;248:162–73.
91. Vu DT, Kieu NM, Tien TQ, Nguyen TP, Vu H, Shin S, Vu NH. Solar concentrator bio-inspired by the superposition compound eye for high-concentration photovoltaic system up to thousands fold factor. *Energies.* 2022;15:3406.
92. Xuan Q, Li G, Lu Y, Zhao B, Zhao X, Su Y, Ji J, Pei G. Overall detail comparison for a building integrated concentrating photovoltaic/daylighting system. *Energy Build.* 2019;199:415–26.
93. Vu H, Tien TQ, Park J, Cho M, Vu NH, Shin S. Waveguide concentrator photovoltaic with spectral splitting for dual land use. *Energies.* 2022;15:2217.
94. Praveenkumar S, Gulakhmadov A, Kumar A, Safaraliev M, Chen X. Comparative analysis for a solar tracking mechanism of solar PV in five different climatic locations in south Indian states: a techno-economic feasibility. *Sustainability.* 2022;14:11880.
95. Melo KB, Moreira HS, Villalva MG. Influence of solar position calculation methods applied to horizontal single-axis solar trackers on energy generation. *Energies.* 2020;13:3826.
96. Riad A, Zohra MB, Alhamany A, Mansouri M. Bio-sun tracker engineering self-driven by thermo-mechanical actuator for photovoltaic solar systems. *Case Stud Therm Eng.* 2020;21:100709.
97. Yakubu RO, Mensah LD, Quansah DA, Adaramola MS. Improving solar photovoltaic installation energy yield using bifacial modules and tracking systems: an analytical approach. *Adv Mech Eng.* 2022;14:1–12.
98. Baouche FZ, Abderezzak B, Ladmi A, Arbaoui K, Suci G, Mihaltan TC, Raboaca MS, Hudisteanu SV, Turcanu FE. Design and simulation of a solar tracking system for PV. *Appl Sci.* 2022;12:9682.
99. Fathabadi H. Comparative study between two novel sensorless and sensor based dual-axis solar trackers. *Sol Energy.* 2016;138:67–76.
100. Babics M, Bastiani MD, Balawi AH, Ugur E, Aydin E, Subbiah AS, Liu J, Azmi L, Xu R, Allen TG, Rehman A, Altmann T, Salvador MF, Wolf SD. Unleashing the full power of perovskite/silicon tandem modules with solar trackers. *ACS Energy Lett.* 2022;7:1604–10.
101. Martínez-García E, Blanco-Marigorta E, Gayo JP, Navarro-Manso A. Influence of inertia and aspect ratio on the torsional galloping of single-axis solar trackers. *Eng Struct.* 2021;243:112682.
102. Valentín D, Valero C, Egusquiza M, Presas A. Failure investigation of a solar tracker due to wind-induced torsional galloping. *Eng Fail Anal.* 2022;135:106137.
103. Ma W, Zhang W, Zhang X, Chen W, Tan Q. Experimental investigations on the wind load interference effects of single-axis solar tracker arrays. *Renew Energy.* 2023;202:566–80.
104. Kuttybay N, Saymbetov A, Mekhilef S, Nurgaliyev M, Tukymbekov D, Dosymbetova G, Meirkhanov A, Svanbayev Y. Optimized single-axis schedule solar tracker in different weather conditions. *Energies.* 2020;13:5226.
105. Gómez-Uceda FJ, Moreno-García IM, Jiménez-Martínez JM, López-Luque R, Fernández-Ahumada LM. Analysis of the influence of terrain orientation on the design of PV facilities with single-axis trackers. *Appl Sci.* 2020;10:8531.
106. Chu CR, Tsao SJ. Aerodynamic loading of solar trackers on flat-roofed buildings. *J Wind Eng Ind Aerodyn.* 2018;175:202–12.
107. de Sá Campos MH, Tiba C. npTrack: a n-position single axis solar tracker model for optimized energy collection. *Energies.* 2021;14:925.
108. Jaouhari ZE, Zaz Y, Moughyt S, Kadmiri OE, Kadmiri ZE. Dual-axis solar tracker design based on a digital hemispherical imager. *J Sol Energy Eng.* 2019;141:011001.
109. Wu CH, Wang HC, Chang HY. Dual-axis solar tracker with satellite compass and inclinometer for automatic positioning and tracking. *Energy Sustain Dev.* 2022;66:308–18.
110. Satué MG, Castaño F, Ortega MG, Rubio FR. Auto-calibration method for high concentration sun trackers. *Sol Energy.* 2020;198:311–23.
111. Dahlioui D, Alaoui SM, Laarabi B, Barhdadi A. Waterless cleaning technique for photovoltaic panels on dual-axis tracker. *Environ Sci Pollut Res.* 2023;30:81667–85.
112. Gönül Ö, Yazar F, Can Duman A, Güler Ö. A comparative techno-economic assessment of manually adjustable tilt mechanisms and automatic solar trackers for behind-the-meter PV applications. *Renew Sustain Energy Rev.* 2022;168:112770.
113. Badr F, Radwan A, Ahmed M, Hamed AM. Performance assessment of a dual-axis solar tracker for concentrator photovoltaic systems. *Int J Energy Res.* 2022;46:13424–40.
114. Hua Z, Ma C, Lian J, Pang X, Yang W. Optimal capacity allocation of multiple solar trackers and storage capacity for utility-scale photovoltaic plants considering output characteristics and complementary demand. *Appl Energy.* 2019;238:721–33.
115. Hammoumi AE, Motahhir S, Ghzizal AE, Chalh A, Derouch A. A simple and low-cost active dual-axis solar tracker. *Energy Sci Eng.* 2018;6:1–14.
116. Daneshazarian R, Cuce E, Cuce PM, Sher F. Concentrating photovoltaic thermal (CPVT) collectors and systems: theory, performance assessment and applications. *Renew Sustain Energy Rev.* 2018;81:473–92.
117. Su Y, Sui P, Davidson JH. A sub-continuous lattice Boltzmann simulation for nanofluid cooling of concentrated photovoltaic thermal receivers. *Renew Energy.* 2022;184:712–26.
118. Wang H, Qu J, Sun Q, Kang Z, Han X. Thermal characteristic comparison of three-dimensional oscillating heat pipes with/without sintered copper particles inside flat-plate evaporator for concentrating photovoltaic cooling. *Appl Therm Eng.* 2020;167:114815.
119. Tan WC, Saw LH, Yusof F, Thiam HS, Xuan J. Investigation of functionally graded metal foam thermal management system for solar cell. *Int J Energy Res.* 2019;44:1–17.
120. Agyekum EB, PraveenKumar S, Alwan NT, Velkin VI, Shcheklein SE. Effect of dual surface cooling of solar photovoltaic panel on the efficiency of the module: experimental investigation. *Helvion.* 2021;7:e07920.
121. PraveenKumar S, Agyekum EB, Alwan NT, Velkin VI, Yaqoob SJ, Adebayo TS. Thermal management of solar photovoltaic module to enhance output performance: an experimental passive cooling approach using discontinuous aluminium heat sink. *Int J Renew Energy Res.* 2021;11:1700–12.
122. Nižetić S, Giama E, Papadopoulos AM. Comprehensive analysis and general economic-environmental evaluation of cooling techniques for photovoltaic panels, Part II: active cooling techniques. *Energy Convers Manag.* 2018;155:301–23.
123. Zubeer SA, Ali OM. Performance analysis and electrical production of photovoltaic modules using active cooling system and reflectors. *Ain Shams Eng J.* 2021;12:2009–16.
124. Islam K, Riggs B, Ji Y, Robertson J, Spitler C, Romanin V, Codd D, Escarra MD. Transmissive microfluidic active cooling for concentrator photovoltaics. *Appl Energy.* 2019;236:906–15.
125. Sargunanathan S, Elango A, Tharves Mohideen S. Performance enhancement of solar photovoltaic cells using effective cooling methods: a review. *Renew Sustain Energy Rev.* 2016;64:382–93.
126. Gomaa MR, Al-Dhaifallah M, Alahmer A, Rezk H. Design, modeling, and experimental investigation of active water cooling concentrating photovoltaic system. *Sustainability.* 2020;12:5392.

127. Wang Y, Huo J, Zhou L, Huang Q. Comparative study of high concentrating photovoltaics integrated with phase-change liquid film cooling system. *Int J Energy Res.* 2019;43:1–15.
128. Acar B, Gürel AE, Ergün A, Ceylan I, Ağbulut Ü, Can A. Performance assessment of a novel design concentrated photovoltaic system coupled with self-cleaning and cooling processes. *Environ Prog Sustain Energy.* 2020;39:e13416.
129. Sharma MK, Bhattacharya J. Finding optimal operating point for advection-cooled concentrated photovoltaic system. *Sustain Energy Technol Assess.* 2022;49:101769.
130. Radwan A, Ookawara S, Ahmed M. Analysis and simulation of concentrating photovoltaic systems with a microchannel heat sink. *Sol Energy.* 2016;136:35–48.
131. Jowkar S, Shen X, Olyaei G, Morad MR, Zeraatkardevin A. Numerical analysis in thermal management of high concentrated photovoltaic systems with spray cooling approach: a comprehensive parametric study. *Sol Energy.* 2023;250:150–67.
132. Yu H, Zhuang J, Li T, Li W, He T, Mao N. Influence of transient heat flux on boiling flow pattern in a straight microchannel applied in concentrator photovoltaic systems. *Int J Heat Mass Transf.* 2022;190:122792.
133. Wu Y, Cui J, Xu X, Deng D. Experimental study on active cooling for concentrating photovoltaic cells working at high concentration ratios. *Int J Energy Res.* 2021;45:1–14.
134. Varghese D, Alnaimat F, Mathew B. Characteristics of MEMS heat sink using serpentine microchannel for thermal management of concentrated photovoltaic cells. *IEEE Access.* 2023;11:10483–98.
135. Ansari D, Jeong JH. A novel variable-height-pinfin isothermal heat sink for densely-packed concentrated photovoltaic systems. *Energy Convers Manag.* 2022;258:115519.
136. Xiao Y, Bao Y, Yu L, Zheng X, Qin G, Chen M, He M. Ultra-stable carbon quantum dot nanofluids as excellent spectral beam splitters in PV/T applications. *Energy.* 2023;273:127159.
137. Sun L, Yang L, Zhao N, Song J, Li X, Wu X. A review of multifunctional applications of nanofluids in solar energy. *Powder Technol.* 2022;411:117932.
138. Zou Y, Qin CY, Zhai H, Sun CL, Zhang B, Wu XH. The optical characteristics of C@Cu core-shell nanorods for solar thermal applications. *Int J Therm Sci.* 2022;182:107824.
139. Ahmed A, Baig H, Sundaram S, Mallick TK. Use of nanofluids in solar PV/thermal systems. *Int J Photoenergy.* 2019;2019:1–17.
140. Das L, Rubbi F, Habib K, Aslfattahi N, Rahman S, Yahya SM, Kadrigama K. Insight into the investigation of diamond nanoparticles suspended Thermol@55 nanofluids on concentrated photovoltaic/thermal solar collector. *Nanomaterials.* 2022;12:2975.
141. Elminshawy N, Elminshawy A, Osama A, Bassyouni M, Arıcı M. Experimental performance analysis of enhanced concentrated photovoltaic utilizing various mass flow rates of Al<sub>2</sub>O<sub>3</sub>-nanofluid: energy, exergy, and exergoeconomic study. *Sustain Energy Technol Assess.* 2022;53:102723.
142. Rubbi F, Das L, Habib K, Saidur R, Yahya SM, Aslfattahi N. MXene incorporated nanofluids for energy conversion performance augmentation of a concentrated photovoltaic/thermal solar collector. *Int J Energy Res.* 2022;46:24301–21.
143. Salem H, Mina E, Abdelmessih R, Mekhail T. Numerical investigation for performance enhancement of photovoltaic cell by nanofluid cooling. *J Sol Energy Eng.* 2022;144:021012.
144. Elminshawy NAS, El-Ghandour M, Elhenawy Y, Bassyouni M, Damhogi DG, El-Addas MF. Experimental investigation of a V-trough PV concentrator integrated with a buried water heat exchanger cooling system. *Sol Energy.* 2019;193:706–14.
145. Ji Y, Artzt LE, Adams W, Spittler C, Islam K, Codd D, Escarra MD. A transmissive concentrator photovoltaic module with cells directly cooled by silicone oil for solar cogeneration systems. *Appl Energy.* 2021;288:116622.
146. Lashin A, Turkestani MA, Sabry M. Performance of a thermo-electric generator partially illuminated with highly concentrated light. *Energies.* 2020;13:3627.
147. Praveenkumar S, Gulakhmadov A, Agyekum EB, Alwan TN, Velkin VI, Sharipov P, Safaraliev M, Chen X. Experimental study on performance enhancement of a photovoltaic module incorporated with CPU heat pipe—a 5E analysis. *Sensors.* 2022;22:6367.
148. Luo Q, Li P, Cai L, Chen X, Yan H, Zhu H, Zhai P, Li P, Zhang Q. Experimental investigation on the heat dissipation performance of flared-fin heat sinks for concentration photovoltaic modules. *Appl Therm Eng.* 2019;157:113666.
149. Alzahrani M, Baig H, Shanks K, Mallick T. Estimation of the performance limits of a concentrator solar cell coupled with a micro heat sink based on a finite element simulation. *Appl Therm Eng.* 2020;176:115315.
150. Song Z, Ji J, Zhang Y, Cai J, Li Z, Li Y. Mathematical and experimental investigation about the dual-source heat pump integrating low concentrated photovoltaic and finned-tube exchanger. *Energy.* 2023;263:125690.
151. Youssef R, Hosen MS, He J, Al-Saadi M, Mierlo JV, Berecibar M. Novel design optimization for passive cooling PCM assisted battery thermal management system in electric vehicles. *Case Stud Therm Eng.* 2022;32:101896.
152. Abdollahi N, Rahimi M. Potential of water natural circulation coupled with nano-enhanced PCM for PV module cooling. *Renew Energy.* 2020;147:302–9.
153. Aslfattahi N, Saidur R, Arifutzzaman A, Abdelrazik AS, Samylingam L, Sabri MFM, Sidik NAC. Improved thermo-physical properties and energy efficiency of hybrid PCM/graphene-silver nanocomposite in a hybrid CPV/thermal solar system. *J Therm Anal Calorim.* 2022;147:1125–42.
154. Rejeb O, Lamrani B, Lamba R, Kousksou T, Salameh T, Jemni A, Hamid AK, Bettayeb M, Ghenai C. Numerical investigations of concentrated photovoltaic thermal system integrated with thermoelectric power generator and phase change material. *J Energy Storage.* 2023;62:106820.
155. Yusuf A, Ballikaya S. Performance analysis of concentrated photovoltaic systems using thermoelectric module with phase change material. *J Energy Storage.* 2023;59:106544.
156. Sharma S, Sellami N, Tahir AA, Mallick TK, Bhakar R. Performance improvement of a CPV system: experimental investigation into passive cooling with phase change materials. *Energies.* 2021;14:3550.
157. Sabry M, Lashin A. Performance of a heat-pipe cooled concentrated photovoltaic/thermoelectric hybrid system. *Energies.* 2023;16:1438.
158. Shittu S, Li G, Zhao X, Akhlaghi YG, Ma X, Yu M. Comparative study of a concentrated photovoltaic–thermoelectric system with and without flat plate heat pipe. *Energy Convers Manag.* 2019;193:1–14.
159. Wang Y, Hu G, Cui Y, Huang Q. Experimental study on cooling performance of solar cells with atmospheric plate thermosyphon. *Energy Convers Manag.* 2018;178:226–34.
160. Soliman AMA, Hassan H. An experimental work on the performance of solar cell cooled by flat heat pipe. *J Therm Anal Calorim.* 2021;146:1883–92.
161. Stevens KA, Smith SM, Taft BS. Variation in oscillating heat pipe performance. *Appl Therm Eng.* 2019;149:987–95.
162. Okazaki S, Fuke H, Ogawa H. Performance of circular oscillating heat pipe for highly adaptable heat transfer layout. *Appl Therm Eng.* 2021;198:117497.

163. Patel V, Mehta N, Mehta K, Badgujar A, Mehta S, Bora N. Experimental investigation of flat plate cryogenic oscillating heat pipe. *J Low Temp Phys*. 2020;198:41–55.
164. Agyekum EB, PraveenKumar S, Alwan NT, Velkin VI, Adebayo TS. Experimental study on performance enhancement of a photovoltaic module using a combination of phase change material and aluminum fins—exergy, energy and economic (3E) analysis. *Inventions*. 2021;6:69.
165. Agyekum EB, PraveenKumar S, Alwan NT, Velkin VI, Shcheklein SE, Yaqoob SJ. Experimental investigation of the effect of a combination of active and passive cooling mechanism on the thermal characteristics and efficiency of solar PV module. *Inventions*. 2021;6:63.
166. Ji Y, Lv S, Qian Z, Ji Y, Ren J, Liang K, Wang S. Comparative study on cooling method for concentrating photovoltaic system. *Energy*. 2022;253:124126.
167. Kouravand A, Kasaeian A, Pourfayaz F, Rad MAV. Evaluation of a nanofluid-based concentrating photovoltaic thermal system integrated with finned PCM heatsink: an experimental study. *Renew Energy*. 2022;201:1010–25.
168. Soliman AMA, Hassan H. Effect of heat spreader size, micro-channel configuration and nanoparticles on the performance of PV-heat spreader-microchannels system. *Sol Energy*. 2019;182:286–97.
169. Nasef HA, Nada SA, Hassan H. Integrative passive and active cooling system using PCM and nanofluid for thermal regulation of concentrated photovoltaic solar cells. *Energy Convers Manag*. 2019;199:11206.
170. Rahmanian S, Rahmanian-Koushkaki H, Omidvar P, Shahsavari A. Nanofluid-PCM heat sink for building integrated concentrated photovoltaic with thermal energy storage and recovery capability. *Sustain Energy Technol Assess*. 2021;46:101223.
171. Torbatinezhad A, Ranjbar AA, Rahimi M, Gorzin M. A new hybrid heatsink design for enhancement of PV cells performance. *Energy Rep*. 2022;8:6764–78.
172. Torbatinezhad A, Rahimi M, Ranjbar AA, Gorzin M. Performance evaluation of PV cells in HCPV/T system by a jet impingement/mini-channel cooling scheme. *Int J Heat Mass Transf*. 2021;178:121610.
173. Tohidi F, Holagh SG, Chitsaz A. Thermoelectric generators: a comprehensive review of characteristics and applications. *Appl Therm Eng*. 2022;201:117793.
174. Sabry M, Lashin A, Turkestani MA. Experimental and simulation investigations of CPV/TEG hybrid system. *J King Saud Univ Sci*. 2021;33:101321.
175. Lekbir A, Hassani S, Mekhilef S, Saidur R, Ghani MRA, Gan CK. Energy performance investigation of nanofluid-based concentrated photovoltaic/thermal-thermoelectric generator hybrid system. *Int J Energy Res*. 2021;45:9039–57.
176. Rodrigo PM, Valera A, Fernández EF, Almonacid FM. Performance and economic limits of passively cooled hybrid thermoelectric generator-concentrator photovoltaic modules. *Appl Energy*. 2019;238:1150–2116.
177. Hajji M, Labrim H, Benaissa M, Faddouli A, Hartiti B, Ez-Zahraouy H. Efficient cooling system for an indirectly coupled CPV-CTE hybrid system. *Int J Energy Res*. 2021;45:1–16.
178. Lekbir A, Hassani S, Ghani MRA, Gan CK, Mekhilef S, Saidur R. Improved energy conversion performance of a novel design of concentrated photovoltaic system combined with thermoelectric generator with advance cooling system. *Energy Convers Manag*. 2018;177:19–29.
179. Brekke N, Dale J, DeJarnette D, Hari P, Orosz M, Roberts K, Tunkara E, Otanicar T. Detailed performance model of a hybrid photovoltaic/thermal system utilizing selective spectral nanofluid absorption. *Renew Energy*. 2018;123:683–93.
180. Kong X, Zhang L, Xu W, Li H, Kang Y, Wu J, Fan M. Performance comparative study of a concentrating photovoltaic/thermal phase change system with different heatsinks. *Appl Therm Eng*. 2022;208:118223.
181. Rejeb O, Shittu S, Li G, Ghenai C, Zhao X, Ménézo C, Jemni A, Jomaa M, Bettayeb M. Comparative investigation of concentrated photovoltaic thermal-thermoelectric with nanofluid cooling. *Energy Convers Manag*. 2021;235:113968.
182. Alzahrani M, Roy A, Shanks K, Sundaram S, Mallick TK. Graphene as a pre-illumination cooling approach for a concentrator photovoltaic (CPV) system. *Sol Energy Mater Sol Cells*. 2021;222:110922.
183. Kumar S, Chander N, Gupta VK, Kukreja R. Progress, challenges and future prospects of plasmonic nanofluid based direct absorption solar collectors—a state-of-the-art review. *Sol Energy*. 2021;227:365–425.
184. Liew NJY, Holman Z, Yu Z, Lee HJ. Application of spectral beam splitting using wavelength-selective filters for Photovoltaic/Concentrated solar power hybrid plants. *Appl Therm Eng*. 2022;201:117823.
185. Han X, Zhao X, Chen X. Design and analysis of a concentrating PV/T system with nanofluid based spectral beam splitter and heat pipe cooling. *Renew Energy*. 2020;162:55–70.
186. Meraje WC, Huang CC, Barman J, Huang CY, Jeffrey Kuo CF. Design and experimental study of a Fresnel lens-based concentrated photovoltaic thermal system integrated with nanofluid spectral splitter. *Energy Convers Manag*. 2022;258:115455.
187. Lin J, Liu S, Ju X, Xu C, Ju X, Liu H. Investigation of two-stage concentrating splitting photovoltaic/thermal system with a flexible heat-electricity ratio based on nanofluid. *Energy Convers Manag*. 2022;258:115531.
188. Anand B, Murugavel S. A hybrid system for power, desalination, and cooling using concentrated photovoltaic/thermal collector. *Energy Source Part A*. 2019;44:1416–36.

**Publisher's Note** Springer Nature remains neutral with regard to jurisdictional claims in published maps and institutional affiliations.

Springer Nature or its licensor (e.g. a society or other partner) holds exclusive rights to this article under a publishing agreement with the author(s) or other rightsholder(s); author self-archiving of the accepted manuscript version of this article is solely governed by the terms of such publishing agreement and applicable law.